Adsorption mechanism of bone chars for defluoridation of groundwater

Miss Benyapa Sawangjang

A Thesis Submitted in Partial Fulfillment of the Requirements
for the Degree of Master of Science Program in Hazardous Substance and
Environmental Management
(Interdisciplinary Program)
Graduate School
Chulalongkorn University
Academic Year 2015

กลไกการดูดซับฟลูออไรด์โดยถ่านกระดูกออกจากน้ำใต้ดิน

นางสาวเบญญาภา สว่างแจ้ง

วิทยานิพนธ์นี้เป็นส่วนหนึ่งของการศึกษาตามหลักสูตรปริญญาวิทยาศาสตรมหาบัณฑิต
สาขาวิชาการจัดการสารอันตรายและสิ่งแวดล้อม (สหสาขาวิชา)
บัณฑิตวิทยาลัย จุฬาลงกรณ์มหาวิทยาลัย
ปีการศึกษา 2558

Thesis Title	Adsorption mechanism of bone chars for defluoridation of groundwater
By	Miss Benyapa Sawangjang
Field of Study	Hazardous Substance and Environmental Management
Thesis Advisor	Aunnop Wongrueng, Ph.D.
Thesis Co-Advisor	Professor Eakalak Khan, Ph.D.

Accepted by the Graduate School, Chulalongkorn University in Partial Fulfillment of the Requirements for the Master's Degree

.....Dean of the Graduate School
(Associate Professor Sunait Chutintaranond, Ph.D.)

THESIS COMMITTEE

.....Chairman
(Assistant Professor Chantra Tongcumpou, Ph.D.)

.....Thesis Advisor
(Aunnop Wongrueng, Ph.D.)

.....Thesis Co-Advisor
(Professor Eakalak Khan, Ph.D.)

.....Examiner
(Associate Professor Patiparn Punyapalakul, Ph.D.)

.....External Examiner
(Athit Phetrak, Ph.D.)

เบญญาภา สว่างแจ้ง : กลไกการดูดซับฟลูออไรด์โดยถ่านกระดูกออกจากน้ำใต้ดิน (Adsorption mechanism of bone chars for defluoridation of groundwater) อ.ที่ปรึกษาวิทยานิพนธ์หลัก: ดร.อรรณพ วงศ์เรือง, อ.ที่ปรึกษาวิทยานิพนธ์ร่วม: ศ. ดร. เอกลักษณ์ คาน, หน้า.

งานวิจัยนี้มีจุดประสงค์เพื่อศึกษากลไกการดูดซับฟลูออไรด์โดยใช้ ถ่านกระดูกหมู ถ่านกระดูกไก่และถ่านกระดูกวัว ซึ่งถ่านกระดูกทั้ง 3 ชนิด จะถูกสังเคราะห์ได้โดยการบวนการผ่านความร้อนที่อุณหภูมิสูง และสารไฮดรอกซีอะพาไทต์ส่วนประกอบหลักของถ่านกระดูก งานวิจัยนี้ได้ดำเนินการตรวจสอบคุณสมบัติทางกายภาพด้วยเทคนิค XRD และ BET ผลจากการทดลองของ XRD ถ่านกระดูกหมูเป็นตัวดูดซับที่สามารถผลิตสารไฮดรอกซีอะพาไทต์ได้มากที่สุดเมื่อเทียบกับตัวดูดซับที่เหลือ สำหรับผลการทดลองของ BET ทำให้ทราบว่าถ่านกระดูกวัวมีพื้นที่ผิวมากที่สุดเมื่อเทียบกับถ่านกระดูกตัวอื่น อีกทั้ง แรงดึดดูดไฟฟ้าสถิตเป็นกลไกหลักในการดูดติดระหว่างผิวของถ่านกระดูกและฟลูออไรด์ จากนั้นทำการศึกษากลไกการดูดซับแบบจลนพลศาสตร์และไอโซเทอม การดูดซับฟลูออไรด์โดยใช้ถ่านกระดูกทั้ง 3 ตัวจะเข้าสู่สภาวะสมดุลเมื่อเวลาสัมผัสมากกว่า 3 ชั่วโมง อีกทั้ง ผลการทดลองนี้ยังสามารถสรุปได้ว่าถ่านกระดูกทั้ง 3 ชนิด สอดคลองกับ สมการปฏิกิริยาอันดับสองเทียมและไอโซเทอมของการดูดซับสอดคล้องกับสมการแลงเมียร์

นอกจากนี้ งานวิจัยนี้ได้ทำการศึกษาผลกระทบของความเป็นกรด-ด่าง ของน้ำ และประจุลบอื่นที่มีผลต่อการดูดซับของฟลูออไรด์โดยใช้ถ่านกระดูก จากผลการทดลอง ความเป็นกรด-ด่างส่งผลกระทบต่อการลดลงของการดูดซับฟลูออไรด์โดยถ่านกระดูกมากที่สุดเมื่อเทียบกับสภาวะแวดล้อมอื่น นอกจากนี้ ประสิทธิภาพในการกำจัดฟลูออไรด์โดยใช้ถ่านกระดูกจะลดลงเมื่อนำกระดูกไปใช้กับน้ำสังเคราะห์ที่ถูกปนเปื้อนด้วยฟลูออไรด์

สาขาวิชา การจัดการสารอันตรายและสิ่งแวดล้อม ลายมือชื่อนิสิต .....

ปีการศึกษา 2558 ลายมือชื่อ อ.ที่ปรึกษาหลัก .....

ลายมือชื่อ อ.ที่ปรึกษาร่วม .....

5787565720 : MAJOR HAZARDOUS SUBSTANCE AND ENVIRONMENTAL MANAGEMENT

KEYWORDS: ADSORPTION PROCESS / BONE CHAR / FLUORIDE / HYDROXYAPATITE / LANGMUIR ISOTHERM / PSEUDO-SECOND ORDER

BENYAPA SAWANGJANG: Adsorption mechanism of bone chars for defluoridation of groundwater. ADVISOR: AUNNOP WONGRUENG, Ph.D., CO-ADVISOR: PROF. EAKALAK KHAN, Ph.D., pp.

The purpose of the research was to examine the adsorption fluoride onto pig bone char (PBC), chicken bone char (CKBC), and cow bone char (CBC) adsorbents. Bone char (BC) adsorbents were generated by charring process. The BC synthesis was characterized the physicochemical properties by X-ray diffraction (XRD) and N_2 adsorption-desorption isotherm. According to the XRD result, PBC could produce higher percentage of hydroxyapatite (HAP) than those of CKBC and CBC adsorbents. Furthermore, the electrostatic interaction between BC surface and fluoride ion was dominant mechanism.

The adsorption kinetics and adsorption isotherms were examined under batch condition. Along with the kinetic study, the adsorption fluoride on all of adsorbents reached to the equilibrium after 3 hours of contact time. The pseudo-second order model was found to fit well with the fluoride adsorption kinetic of all adsorbents. According to the adsorption isotherm result, all adsorbents showed adsorption isotherm, which best fitted with Langmuir isotherm model.

The result reveled that the adsorption of fluoride on BC synthesized adsorbents affected by pH solution and anions. In addition, Low fluoride removal efficiency was observed when synthetic water of fluoride was used.

Field of Study: Hazardous Substance and Environmental Management

Student's Signature .....

Advisor's Signature .....

Co-Advisor's Signature .....

Academic Year: 2015

ACKNOWLEDGEMENTS

Firstly, I would like to express my sincere gratitude to my advisor and co-advisor; Dr.Aunnop Wongrueng and Prof.Dr.Eakalak Khan for their continuous support and helpful suggestion.

Besides, I would like to represent my appreciate to Assst.Prof.Dr.Chantra Tongcumpou, Assoc.Prof.Dr.Patiphan Punyapalakul, and Dr.Athit Phetrak members of my committee for their useful and valuable comments.

I am grateful for the financial support from the Center of Excellence on Hazardous Substance Management, Chulalongkorn University and the Kurita Water and Environment Foundation (KWEF). I also gratefully acknowledge technician support from Department of Environmental Engineering, Faculty of Engineering Chiang Mai University

Finally, I would like to appreciate my family for their support and encouragement. Furthermore, I would like to thanks for my friends and my seniors for their favorable help.

CONTENTS

Page

Page

Page

Page

LIST OF FIGURE

LIST OF TABLE

ABREVIATION

BC	Bone char
°C	Degree Celsius
cal	Calculation
CBC	Cow bone char
CKBC	Chicken bone char
exp	Experiment
F^-	Fluoride
g	gram
H	Hour
HAP	Hydroxyapatite
IC	Inorganic carbon
L	Liter
mg	Milligram
min	minute
mL	Milliliter
N	Normal unit
PBC	Pig bone char

PZC	Point of zero charge
s	Second
TC	Total carbon
TOC	Total organic carbon
UV	Ultraviolet
XRD	X-ray diffraction

CHAPTER 1

INTRODUCTION

1.1 Background

In many areas in the world, groundwater is used to produce drinking water because it is of better quality with less microbial contamination, than surface water. Furthermore, some areas have contaminated surface water and/or limited sources of surface water. However, groundwater sometimes is contaminated naturally because of geochemical characteristics. Fluoride and arsenic are prime examples of naturally occurring contaminants in groundwater.

Fluoride (F^-) has beneficial and detrimental effects, depending on its concentration in drinking water. At low concentrations (0.4-1.0 mg/l), fluoride is beneficial for the teeth of young children, as it is able to protect teeth against decay and promote the calcification of dental enamel (Loganathan, Vigneswaran, Kandasamy, & Naidu, 2013).On the other hand, high concentrations of fluoride over than 1.5 mg/L in groundwater can cause dental and skeletal fluorosis, bone diseases, the mottling of teeth, and lesions on the thyroid, liver and other organs(Jimenez-Reyes & Solache-Rios, 2010). Fluoride is released into groundwater through the dissolution of fluorine in rocks. Furthermore, fluorite, biotites, topaz, geanite, basalt, syenite, and shale are subsurface minerals that can release fluoride into groundwater (Bhatnagar, Kumar, & Sillanpää, 2011)

Fluoride contamination in groundwater has been recognized as a serious environmental problem worldwide. Many countries such as Tunisia, Morocco, Algeria, and Senegal encounter excessive fluoride in drinking water (Bhatnagar et al., 2011). Thus, the World Health Organization (WHO) set the maximum level of fluoride in drinking water at 1.5 mg/L . In addition, the populations in the northern part of

Thailand such as Chiang Mai, Lamphun, Mae Hong Son province, have been exposed to high levels of fluoride from drinking water as presented in Figure 1 and Figure 2 (maximum fluoride concentration at 16.1 mg/L). Therefore, the standard of fluoride in drinking water in Thailand established by the Ministry of Public Health is 0.7 mg/L(Thailand, 2002).

Several methods such as adsorption, ion exchange, precipitation, electrodialysis and nanoflitration, can be applied to reduce fluoride in groundwater. Each of these methods has advantages and disadvantages. Adsorption is a method that is more convenient and can be economical depending on the type of adsorbents. Developing countries tend to use simple inexpensive adsorbents that are locally available such as natural adsorbents. On the other hand, in developed countries, more efficient but more costly adsorbents such as activated carbon and synthetic polymers are applied (Loganathan et al., 2013).

Examples of low-cost and effective adsorbents for the removal of fluoride include kaolinite, bentonite, charfine, lignites, sirmali seeds, gas concrete material, alum sludge, alumina, activated charcoal, amorphous alumina, calcite, bleaching earth, red mud, and bone char (Tor, 2006). Bone char (BC) is an alternative material that can treat fluoride in drinking water. However, application of bone char for defluoridation can result in the treated water having an unpleasant taste, smell, and color (yellowish). When charring temperatures are below 500°C; the bone char can still have the remains of some organic matter, which is the major cause of these problems (Leyva-Ramos, Rivera-Utrilla, Medellin-Castillo, & Sanchez-Polo, 2010).

Bone char contains hydroxyapatite, which is a mixture between carbon and calcium phosphate. Bone char is a blackish, porous, granular material and can be generated by heating in a furnace. Bone char can be synthesized by a calcination or pyrolysis method. The calcination of bone is under a low-oxygen environment

condition. Pyrolysis generates bone char with no oxygen present during the thermal treatment (Rojas-Mayorga et al., 2013).

Bone char is 57–80% calcium phosphate in a form of hydroxyapatite ($Ca_{10}(PO_4)_6(OH)_2$), 6–10% calcium carbonate and 7–10% activated carbon. Bone char removes fluoride that contaminates groundwater by replacing the hydroxyl ions with fluoride ions according to the following chemical reaction (Rao, Reddy, Lakshmikanth, & Ambika, 2009).

$$Ca_{10}(PO_4)_6(OH)_2 + 2F^- \rightarrow Ca_{10}(PO_4)_6F_2 + 2OH^-$$

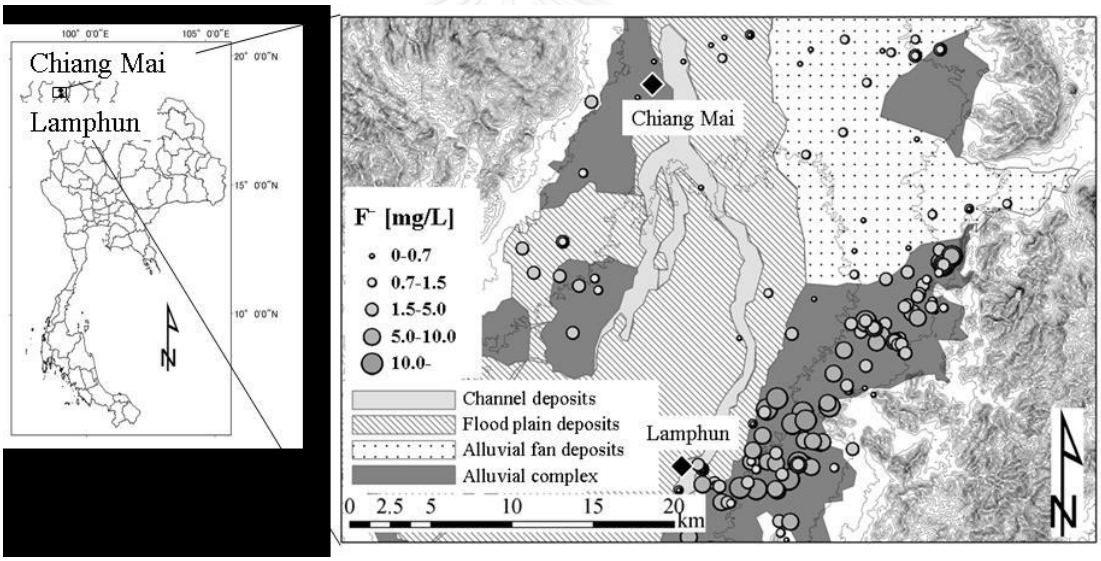

Figure 1 Fluoride concentration in groundwater of northern part of Thailand (Kainosho et al., n.d.)

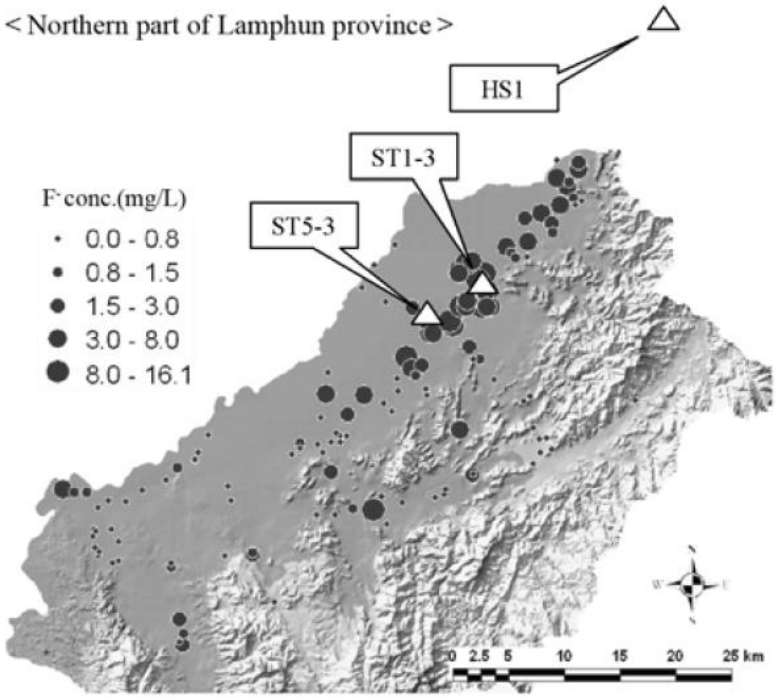

Figure 2 Fluoride concentration in groundwater of Lamphun province (Wongrueng, Takizawa, Matsui, Oguma, & Wattanachira, Received May 23, 2008)

1.2 Objectives

1. To synthesize bone char for the defluoridation of groundwater
2. To compare the efficiency of each bone type for fluoride removal in groundwater
3. To investigate effect of the pyrolysis process (temperature and time), pH, and competitive ions on fluoride adsorption capacity

1.3 Hypotheses

1. Different types of bone applied for the defluoridation of groundwater provide different fluoride removal. Cattle bone gives the highest percent of hydroxyapatite, thus it will has the highest defluoridation efficiency.
2. Different conditions for generating bone char result in different amounts of hydroxyapatite.

3. Bone char, which has the highest percentage of hydroxyapatite and surface area, will have high fluoride removal capacity.

1.4 Scope of the Study

1. Bone char will be synthesized using cattle, pig and chicken bones.

2. Synthetic contaminated water samples will be made by adding NaF to deionized water.

3. The adsorption experiments will be investigated under a batch condition.

4. Adsorption kinetics will be investigated by varying contact time from 0 to 24 hours. The pseudo-first-order and the pseudo-second-order will be applied to analyze the adsorption rate and mechanisms.

5. Adsorption isotherms will be investigated by varying the initial fluoride concentration. The adsorption isotherms, which are the Langmuir and Fruendlich models, will be examined to determine the adsorption mechanism.

6. The defluoridation process will be conducted in two parts, consisting the synthetic contaminated water and actual contaminated groundwater.

7. Parameters

7.1 Bone char analyses (absorbent)

- Percent hydroxyapatite [X-ray diffraction (XRD) method]
- Surface area [(BET) method]
- Point of zero charge (PZC)

7.2 Water sample analyses

- Adsorption fluoride capacity (UV-6400 SPECTROPHOTOMETER, 570 nm)
- pH
- Competitive anions (Chloride and sulfate ion)

The experiment framework of this research is showed in Figure 3

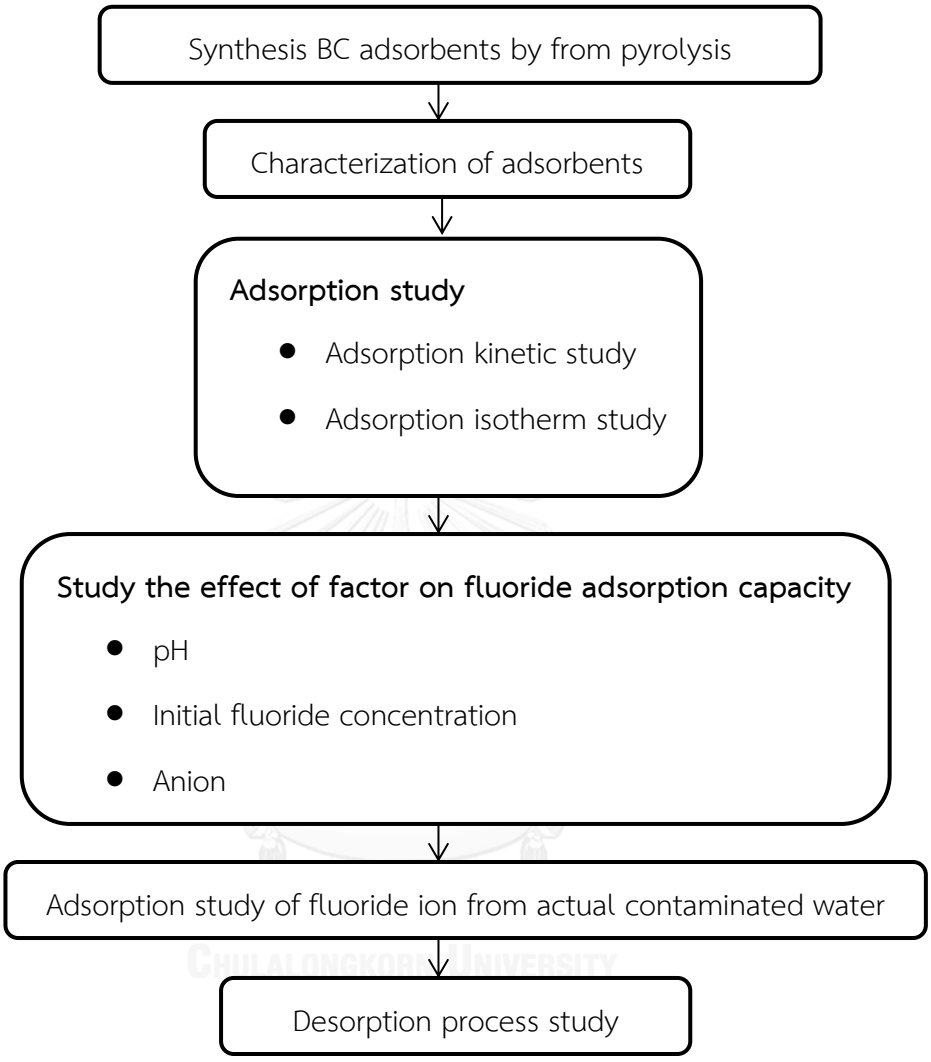

Figure 3 Scope of this study

CHAPTER 2

THEORY BACKGRUONG AND LITERATURE REVIEW

2.1 Fluoride

Fluoride is beneficial and destructive to human health depending on the exposure concentration. The WHO sets the standard level of fluoride concentration in drinking water at 1.5 mg/L. Fluoride in groundwater has been recognized as a serious environmental problem worldwide because groundwater is one of the major raw water sources for drinking water. High fluoride intake can cause a range of adverse health problems such as fluorosis, cancer, destroyed kidney function, digestive system and nervous disorder, reduced immunity, adverse pregnancy outcomes, respiratory problems, thyroid, liver, and other organs. Furthermore, it can affect teeth and bones; issues include the mottling of teeth, the embrittlement of bone, osteoporosis, and arthritis. At least 28 countries worldwide have experienced excessive concentrations of fluoride (Loganathan et al., 2013).

High fluoride concentrations in groundwater are found in several parts of the world. One of the causes is fluoride distribution in subsurface geological materials. It is generally released in the groundwater through the dissolution of fluoride in rocks. In addition, several industrial activities are also creating fluoride pollution to environment because they discharge wastewater containing high fluoride concentrations. Such industries include those involved in glass and ceramic production, semiconductor manufacturing, electroplating, coal fried power, beryllium extraction, brick and iron works, and aluminum (Ben Nasr, Walha, Charcosset, & Ben Amar, 2011).

2.2 Methods for defluoridation

Several studies report various methods for removing fluoride ions in groundwater. The goal is to remove the fluoride concentration in groundwater to below the acceptable level (1.5 mg/L). Thus, some fluoride ions will remain in groundwater after treatment (Loganathan et al., 2013). The main methods for removing fluoride in groundwater are precipitation/coagulation, membrane techniques, and adsorption. Each of these methods has benefits and drawbacks.

2.2.1 Precipitation/Coagulation

Precipitation/Coagulation is the traditional method for removing fluoride in groundwater. It is most widely applied. However, it also has shortcomings such as high operational and maintenance costs, low effectiveness because it cannot remove fluoride to below 5 mg/L, large chemical requirements, and the secondary pollution generated (large volumes of waste sludge) (Ben Nasr et al., 2011).

2.2.2 Membrane techniques

Although membrane techniques can deliver high fluoride removal efficiency, it has major drawbacks on installation, operation, and maintenance costs. The two common membrane techniques are reverse osmosis and electrodialysis.

2.2.2.1 Reverse osmosis

Reverse osmosis can achieve up to 98% rejection of fluoride ions. In addition, this process can be totally regenerated after each set of experiment (Mohapatra, Anand, Mishra, Giles, & Singh, 2009). This process did not need the additional of chemicals and non-ion selectively. On the other hand, it has some limitations: high capital and operation costs; and clogging, scaling, and

fouling problems; and the need for pH control because some membranes are sensitive to pH(Loganathan et al., 2013).

2.2.2.2 Electrodialysis

Electrolysis separates solutes by transporting solutes through a membrane rather than using a membrane to retain the solutes. Furthermore, the membrane pores of electrodialysis are less restrictive than nanofiltration. The solutes can be driven by applying an electric field (Singh, Singh, & Singh, , 2014).The benefits of electrodialysis include high efficiency for fluoride removal, no chemicals required, no waste produced, and no ion selection. However, the process has limitations such as its high operational costs associated with energy requirement, skilled labor requirement, and polarization problems (Loganathan et al., 2013).

2.2.3 Adsorption process

The adsorption process is a widely used and convenient method for defluoridation. The method seems to be more attractive because it presents satisfactory results for removing fluoride in groundwater. In addition, it is a low cost and simple process (for design and operation), and various absorbents both conventional and non-conventional types can be applied (Ben Nasr et al., 2011).

2.2.3.1 Theoretical of absorption

2.2.3.1.1 Adsorption kinetic models

The kinetic models have been investigated for determining the overall adsorption rate of fluoride ions on bone char as a solid adsorbent. The kinetic models were derived by performing a mass balance of the adsorbate (Leyva-Ramos et al., 2010).

$$\mathrm{m}\frac{\mathrm{dq}}{\mathrm{dt}} + \mathrm{V}\frac{\mathrm{dC_A}}{\mathrm{dt}} = 0 \quad (2.1)$$

Solving equation 2.3.1 the amount of fluoride uptakes of bone chars or q_e (mg/g) can be calculated as follows (Rojas-Mayorga et al., 2013).

$$q_{F^-} = \left(\frac{[\mathrm{F^-}]_0 - [\mathrm{F^-}]_f}{m}\right) V \quad (2.2)$$

where C_A is concentration of fluoride in aqueous solution (mg/L), T is time (min) $[F^-]_0$ is the initial fluoride concentration (mg/L), $[F^-]_f$ is the final fluoride concentration in the adsorption experiment (mg/L), *m* is the mass of bone char of each type (g), and *V* is the volume of the fluoride solution (L).

This research will apply pseudo-first-order and pseudo-second-order kinetics for describing the adsorption rate of the reaction.

2.2.3.1.1.1 Pseudo-first-order kinetics

The pseudo-first-order model is represented by the following equation

$$\frac{\mathrm{d}q_t}{\mathrm{d}t} = k_{\mathrm{p1}}(q_e - q_t) \quad (2.3)$$

where q_t is the adsorption capacity at time t (mg/g), q_e is the adsorption capacity at equilibrium (mg/g), t is time (min), and k_{p1} is the pseudo-first-order rate constant for the kinetic model (min^{-1}) (Cai et al., 2015).

The pseudo-first-order equation can be rearranged by integrating with the boundary conditions of q_t = 0 at t = 0 and q_t = q_t at t = t, and expressed as the following equation

$$\ln\left(\frac{q_e}{q_e - q_t}\right) = k_{\mathrm{p1}} t \tag{2.4}$$

which can be rearranged as follows

$$\log(q_e - q_t) = \log q_e - \frac{k_{\mathrm{p1}}}{2.303} t \tag{2.5}$$

A linear plot of log (q_e - q_t) versus t provides the value of k_{p1}, which is the slope of the line.

2.2.3.1.1.2 Pseudo-second-order kinetics.

The pseudo-second-order kinetic model is based on an assumption related to the process of chemisorption. It consists of valence forces though sharing or exchange of electron between the sorbent and sorbate. The pseudo-second-order kinetic model is the best fit for adsorption because it is generally applied to describe the chemical reactions of heterogeneous materials (Jimenez-Reyes & Solache-Rios, 2010). This model is represented by the following equation

$$\frac{\mathrm{d}q_t}{\mathrm{d}t} = k_{\mathrm{p2}}(q_e - q_t)^2 \tag{2.6}$$

where q_t is the adsorption capacity at time t, (mg/g), q_e is the adsorption capacity at equilibrium (mg/g), t is time (h), and k_{p2} is the pseudo-second-order rate constant for the kinetic model (g/mg•h); which can be rearranged as follows

$$\frac{\mathrm{d}q_t}{(q_e - q_t)^2} = k_{\mathrm{p2}} dt \tag{2.7}$$

Integrating the preceding equation at conditions of $q_t = 0$ at t = 0 and $q_t = q_t$ at t = t, results in equation 2.3.8.

$$\frac{1}{(q_e - q_t)} = \frac{1}{q_e} + k_{\mathrm{p2}} t \tag{2.8}$$

which can be rearranged in a linear form as follows

$$\frac{t}{q_t} = \frac{1}{\mathrm{k_{p2}} q_e^2} + \frac{t}{q_e} \tag{2.9}$$

The plot of t/q_t versus t will have a linear tendency, after that the $1/q_e$ value can be obtained from the slope of the line. Thus, k_{p2} can be calculated from the linear equation of the pseudo-second-order.

$$slope = \frac{1}{q_e} \tag{2.10}$$

$$Intercept = \frac{1}{k_{p2} q_e^2} \tag{2.11}$$

2.2.3.1.2 Absorption isotherm models

The optimum conditions for the maximum fluoride removal by bone char can be derived from equilibrium studies. Mathematical models (isotherms) are available for describing sorption behavior of the fluoride ions by bone char at equilibrium.

2.2.3.1.2.1. Linear model

The linear model is expressed by the following equation

$$q_e = K_P C_e \tag{2.12}$$

where q_e is the total amount of fluoride ions sorbed per unit weight of bone char at equilibrium (mg/g), C_e is the concentration of the fluoride ions in the solution at equilibrium (mg/L), and K_P is the constant related to the energy of sorption (L/mg)

2.2.3.1.2.2. Langmuir model

The Langmuir isotherm is the most widely applied with sorption isotherms. This model suits a sorption process where the sorption energy of each molecule is the same, and independent of the surface of the material. In addition, the sorption occurs only on some sites. There are no interactions between the molecules. The model is as follows (Jimenez-Reyes & Solache-Rios, 2010).

$$q_e = \frac{q_0 K_L C_e}{1+K_L C_e} \tag{2.13}$$

where q_0 is the amount of fluoride ions adsorbed per unit weight of bone char in forming a complete monolayer on the surface (mg/g), q_e is the total amount of fluoride ions sorbed per unit weight of bone char at equilibrium (mg/g), C_e is the

concentration of the fluoride ions in the solution at equilibrium (mg/L), and K_L is the constant related to the energy of sorption (L/mg)

The equation of Langmuir model can be linearized as follows

$$\frac{C_e}{q_e} = \frac{1}{q_0 K_L} + \frac{C_e}{q_0} \quad (2.14)$$

$$\frac{1}{q_e} = \frac{1}{K_L q_0}\frac{1}{C_e} + \frac{1}{q_0} \quad (2.15)$$

Based on a plot of $1/q_e$ versus $1/C_e$ has a linear tendeny, $1/(K_L q_o)$ is obtained from the slope and the y intercept is $1/q_0$. Then, K_L can be calculated

When the Langmuir model is applied in the adsorption process, the equilibrium parameter (R_L) should be calculated. It indicates whether the characteristic of the model is consistent or inconsistent with adsorption. R_L can be calculated by the following equation (Piyamungkala, Talwat, Phothimongkonkul, & Kongsompak, 2008)

$$R_L = \frac{1}{1+K_L C_0} \quad (2.16)$$

C_0 is the initial concentration of fluoride ions (mg/L)

Table 1 The type of isotherm based on the equilibrium parameter factor of the Langmuir model (Piyamungkala et al., 2008):

R_L value	Type of isotherm
$R_L > 1$	Unfavorable conditions for sorption
$R_L = 1$	Linear
$0 < R_L < 1$	Favorable conditions for sorption
$R_L = 0$	Irreversible

2.2.3.1.2.3. Freundlich model

The Freundlich isotherm can be applied to non-ideal sorption on heterogeneous surfaces and multilayer sorption. The model is expressed by the following equation (Jimenez-Reyes & Solache-Rios, 2010).

$$q_e = K_F C_e^{1/n} \quad (2.17)$$

Where q_e is the total amount of fluoride ions adsorbed per unit weight of bone char at equilibrium (mg/g), *Ce* is the concentration of the fluoride ions in the solution at equilibrium (mg/L), K_F is the Freundlich constant which can express the capacity of the adsorption process (L/g), and *n* is the Freundlich constant, which explains the concentration of adsorption (dimensionless).

A linear form of the above Freundlich equation is as follows

$$\log q_e = \frac{1}{n}\log C_e + \log K_F \quad (2.18)$$

The slope of a plot log q_e versus log C_e is 1/*n,* which shows the strength between the bone char and fluoride ions, while log K_F is the y-intercept of the plot *(Brunson & Sabatini, 2009).*

Table 2 Characteristic of the Freundlich model based on 1/*n* value (Piyamungkala et al., 2008):

1/*n* value	Characteristic of Freundlich model
1/*n* < 1	The adsorbent has limitation of surface area for adsorption process.

$1/n = 1$	The adsorption isotherm is linear.
$1/n > 1$	The adsorbent has high amount of surface area for adsorption process.

Rojas-Mayorga et al. (2013) reported the Langmuir model being suitable for fluoride removal by adsorption process of bone char. However, Jimenez-Reyes and Solache-Rios (2010) applied hydroxyapatite for adsorbing fluoride ion. They reported the Freundlich model is appropriate for describing the adsorption process of hydroxyapatite. In addition, they revealed the pseudo second order model is the kinetic model that can describe the fluoride sorption by hydroxyapatite. Their findings were supported by Leyva-Ramos et al. (2010).

2.2.3.2 Adsorbent for removing fluoride

Various adsorbents can be used for removing fluoride in groundwater; some of these adsorbents including aluminum, clay and soil, calcium, zeolites, synthetic resins, red mud, carbon, layered double hydroxides, apatite, and hydroxyapatite. A major point of concern in the adsorption process is the cost of the absorbent (Loganathan et al., 2013).

2.2.3.3 Bone char and the process for generating bone char

Bone char application for fluoride removal is a useful, inexpensive, and easy, and a safe and useful way of reusing bone waste (Patel, Han, Qiu, & Gao, 2015). Bone char consists of approximately 75% hydroxyapatite, and 9-11% of calcite and carbon. Hydroxyapatite [Ca_{10} $(PO_4)_6(OH)_2$] is a calcium apatite mineral that is in teeth and bones. Fluoride is removed when the hydroxide component in hydroxyapatite is

replaced by the fluoride ion as shown in the following equation (Brunson & Sabatini, 2009).

$$Ca_{10}(PO_4)_6(OH)_2 + 2F^- \longrightarrow Ca_{10}(PO_4)_6(F)_2 + 2OH^- \quad (2.19)$$

Bone char can be synthetized by pyrolysis or calcination. The calcination of bones is a method that is conducted in a low-oxygen environment while the pyrolysis process is conducted in no oxygen environment. The temperature and residual time for each process play a major role in producing bone char Rojas-Mayorga et al. (2013). When bone char is produced at temperatures below 400°C, the bone char still contains organic matter, which is a major cause of unpleasant taste and odor, and yellow color of treated water. Yet, when bone char is produced at temperatures above 600°C, the apatite structure of bone is destroyed, reducing the functionality of the bone char for the defluoridation process (Brunson & Sabatini, 2009).

The fluoride uptake of bone char generally ranges from 1.0 to 3.0 mg/g of bone char (Rojas-Mayorga et al., 2013). In addition, using bone char as an adsorbent was effective for removing fluoride in groundwater with initial fluoride concentrations ranging 3.5 mg/L to 100 mg/L to less than 0.2 mg/L (Srimurali, Pragathi, & Karthikeyan, 1998). The order of fluoride uptake capacity of various carbon-based adsorbents is bone char > coal charcoal > wood charcoal > carbon black > petroleum coke (Mohapatra et al., 2009).

Dahi and Breghoj (1995) compared the capacities for defluoridation in water by bone char that produced by pyrolysis and calcination. They varied the production temperature (300–800°C) and time (0.5–5 h). The results show that the bone char that was produced by calcination had a lower specific surface area than the bone char that was produced by pyrolysis. Furthermore, the fluoride uptake capacity

drastically decreased when the bone char was produced by calcination at temperatures above 500°C. The best bone char quality was from the pyrolysis process at a temperature up to 700°C at 0.5 h. It is black in color and has the highest fluoride uptake capacity.

Brunson and Sabatini (2009) investigated fish bone char for removing fluoride and arsenic and compared the efficiencies between fish bone char and cow bone char. The results show that the charring temperature affected the capacity and surface area of fish bone char for adsorbing fluoride. The research reports that the charring temperature of 500°C with pyrolysis process is the best temperature for generating bone char providing the highest fluoride efficiency. Furthermore, they observed that the low charring temperature of 300°C was not able to produce favorable results: some organic material was not removed during charring and the specific surface area was 25% of what was observed at higher temperatures. In addition, they reported that fish bone char and cow bone char have minor differences in their fluoride removal capacities.

Rojas-Mayorga et al. (2013) studied how to optimize the pyrolysis process for producing bone char for fluoride removal from water. They observed various adsorption properties of cow bone char that was obtained using different pyrolysis operating conditions. The pyrolysis temperature plays a major role in synthesizing effective bone char for defluoridation. In addition, a charring temperature of 700°C was the best as it generated bone char with the best adsorption properties for fluoride removal. Furthermore, they observed that at temperatures higher than 700 °C, the de-hydroxylation of the hydroxyapatite of the bone char occurred, which reduced its fluoride adsorption capacity. Finally, they reported that the maximum fluoride absorption capacity of bone char obtained was 7.32 mg/g.

Patel et al. (2015) synthesized mesoporous bone chars by pyrolysis. The bone chars were obtained by pyrolyzing bovine and bull bone at 400-600°C. Two pyrolysis

times, 1 and 2 hours, were applied for bone char synthesis. The results show that increasing the pyrolysis temperature and time affected to the microstructure, pore diameter and the crystal size of the bone char. Most of the organics was removed and apatite was obtained by pyrolyzing at 600°C and disappeared as the temperature increased, as confirmed by FTIR and XRD analyses. Finally, they reported that bone char pyrolyzed at 400°C with a residence time of 2 h is a very good low-cost alternative adsorbent because it presents promising physical and chemical characteristics.

2.2.3.4 Factors influencing fluoride adsorption

2.2.3.4.1. Point of zero charge

Wongruwng, Sookwong, Rakruam, and Wattanachira (accepted 2015) reported the PZC of the dolomite sorbent at pH 8.5. At this pH, the dolomite surface was neutral or had a near zero charge. If the pH of solution was above and below this level, the surface of dolomite will be negatively and positively charged, respectively. The dolomite in this study was applied for adsorbing the fluoride ion which is a negative charge ion. Thus, when the pH of solution was lower than 8.5, the adsorption process occurred because the surface charge of dolomite was positive.

Medellin-Castillo et al. (2014)determined the PZC of cattle bone char which is equal to pH = 8.4. In this study, fluoride ion was removed by the electrostatic interactions between the surface charge of bone char and fluoride ion in a water solution. The surface of bone char will attract fluoride ion when the pH of solution lower than 8.4. The fluoride adsorption capacity increased when that the protonation dominated or the pH of solution was lower than PZC level (equation 2.20 and 2.21). On the other hand, the

fluoride adsorption capacity decreased when the deprotonation occurred or the pH of solution was higher than PZC (equation 2.22 and 2.23).

$$\equiv P\text{-}OH + H^{+} \rightarrow \equiv POH_2^{+} \quad (2.20)$$

$$\equiv Ca\text{-}OH + H^{+} \rightarrow \equiv Ca\text{-}OH_2^{+} \quad (2.21)$$

$$\equiv P\text{-}OH \rightarrow \equiv PO^{-} + H^{+} \quad (2.22)$$

$$\equiv Ca\text{-}OH \rightarrow \equiv Ca\text{-}O^{-} + H^{+} \quad (2.23)$$

2.2.3.4.2. The dose of adsorbent and initial fluoride concentration

The relationship between char fine dose and fluoride uptake was studied by Srimurali et al. (1998).They reported that the fluoride uptake increases with adsorbent dose (within a range). When the system had a higher dose of adsorbent, it had more sorbent surface and pore volume available for adsorbing fluoride ion. In addition, the rate of fluoride removal rapidly increased as the initial dose of adsorbent was increased. Above a certain dose range of adsorbent, the rate of fluoride uptake did not significantly increase due to desorption ability of fluoride ions.

2.2.3.4.3. Contact time

Srimurali et al. (1998) reported the capacities of fluoride removal by low cost material at different contact times. The percent of fluoride removal initially increased with contact time. After the system reached the equilibrium state, the increasing of percent removal gradually reduced, eventually leading

to constant removal. Furthermore, after 120 min of contact time, the removal rates eventually decreased to zero level because all adsorbent sites were occupied. After the system attained the equilibrium, the percent of fluoride removal remained relatively stable.

2.2.3.4.4. Co-existing anions that contained in water

Loganathan et al. (2013) concluded that several anions such as PO_4^{3-}, Cl^-, SO_4^{2-}, Br^-, and NO_3^- are able to compete with fluoride ion for removal by some adsorbents. However, the competitive anion will or will not affect the capacity of fluoride removal depending on characteristics of adsorbent and concentration of anions in the solution.

CHAPTER 3

METHODOLOGY

3.1 Materials

3.1.1 Chemical reagents

1.	Acetic acid glacial (CH_3COOH)		RCI Labscan
2.	Barium chloride dihydrate ($BaCl_2$)		EMSURE
3.	Dibasic sodium phosphate ($Na_2HPO_42H_2O$)		MERCK
4.	Diphenylcarbazone		Fluka
5.	Ethanol(Absolute)		RCI Labscan
6.	Hydrochloric acid (HCl)	37%	RCI Labscan
7.	Magnesium chloride ($MgCl_2$·6H2O)		UNIVER
8.	Mercury (II) nitrate monohydrate ($Hg(NO_3)_2·H_2O$)		QRëC
9.	Monobasic sodium phosphate ($NaH_2PO_42H_2O$)		MERCK
10.	Nitic acid (HNO_3)	65%	RCI Labscan
11.	Potassium nitrate (KNO_3)		EMSURE
12.	Sodium acetate trihydrate ($CH_3COOHNa·3H_2O$)		MERCK
13.	Sodium chloride (NaCl)		EMSURE
14.	Sodium fluoride (NaF)		MERCK
15.	Sodium hydroxide (NaOH)		RCI Labscan
16.	Sodium sulfate (Na_2SO_4)		EMSURE
17.	Sulfanilic acid azochromotrop	approx.80%	SIGMA
18.	Sulfuric acid (H_2SO_4)	98%	RCI Labscan
19.	Xylene cyanole FF		SIGMA
20.	Zirconium oxychloride octahydrate ($ZrOCl_2·8H_2O$)		QRëC

3.1.2 Analytical Instruments

1. Raw bone of chicken pig and cow
2. Ceramic cup with lip
3. Deionized water
4. Actual contaminated groundwater from Ban Buak Khang School
5. Tray
6. Foil food wrap
7. Oven
8. Furnace
9. Hammer
10. Crushing machine
11. Sieve 600 μm
12. Membrane filter (Nylon 0.45 μm, 47 mm, wintech)
13. Magnetic stirrer
14. Vacuum filtration apparatus
15. Vacuum pump
16. UV-6400 SPECTROPHOTOMETER, JENWAY
17. pH meter
18. Syringe filter (Nylon 0.45 μm, 13 mm, Chrom tech)
19. Desiccator
20. Plastic bottle 100 mL
21. Shaking machine

3.2 Methods

Research experiments were divided into five steps: testing of various conditions for BC synthesis, characterizations of the BC adsorbent, BC synthesis at the most suitable condition, adsorption study, and defluoridation process study.

3.2.1. Testing of various conditions for BC adsorbent synthesis

Chicken, pig, cow bones were used to produce BC adsorbents which the method for producing it was concluded in Figure 4. Any fat remaining inside the bones were taken out by knife and cleaned by rinsing the bone with deionized water. Then, the clean bones were put in an oven at 110°C for 24 hours to eliminate moisture. Next, the dry bones were crushed by a crushing machine into smaller pieces (around 1-2 inches). After that each type of bone was loaded into a ceramic cup which had a ceramic lid for limiting the amount of oxygen in the charring pyrolysis process. After that, the cup was placed in a furnace which was set at nine different conditions (3 temperatures 450,550, and 650°C and 3 durations ranges: 1, 2, and 3 hours) to produce BC adsorbents.

3.2.2. Characterizations of the adsorbents to identify the most suitable condition for generating BC

The bone chars resulted from the nine production conditions were crushed again by a hammer into a size of sieve No. 60. There were a total of 30 adsorbent samples for 3 bone types, nine samples from the various conditions and a control sample of each type. The controls were the bone that does not undergo the charring process. After that, all the samples were analyzed for the amount of hydroxyapatite by XRD and surface area by the BET method. The charring conditions that produce the highest amount of HAP and the surface area of each bone types were selected

to produce the BC at different suitable conditions of each bone types (pig, chicken, and cow bone).

3.2.3. BC synthesis at the most suitable condition

The most suitable conditions identified in the previous step were applied to produce BC adsorbents for fluoride adsorption study. Then, the best BC of each bone types was obtained in this step.

3.2.4. Adsorption experiment study

The method and instrument for analyzing all parameter in this work were summarized in Table 3.

3.2.4.1 Cleaning BC process

All of bone chars which were obtained from the previous step were cleaned by soaking with deionized water before they were used in an adsorption experiment study. Deionized water for soaking BC was changed every day. Bone chars were soaked for 3 - 4 days until the rinse water was clear. After that, all of them were put in an oven at 110°C for 48 hours to eliminate moisture. Then, the dry BC was kept in a desiccator.

3.2.4.2 PZC determination

A batch equilibrium method was applied for determining the PZC of BC. BC of 0.2 g was shaken with 100 mL of deionized water at 200 rpm for 24 hours and the pH was varied from 3.0 to 12.0 using 0.1 N of nitric acid or 0.1 N of sodium hydroxide. The initial pH was measured before the mixed experiment was started. After 24 hours, the final pH was measured. Then, a relationship between

the initial pH and the final pH was plotted. Finally, the PZC of bone char was obtained from the common plateau of the plot (Babic´, Milonjic´, Polovina, & Kaludierovic, 1999).

3.2.4.3 Contaminated water sample synthesis

Using deionized water mixed with NaF by preparing the stock of water sample around 100 mg/L. Then, a contaminated water sample was diluted into 10 - 25 mg/L of fluoride concentration that used for fluoride adsorption study.

3.2.4.4 Adsorption kinetic study

The absorption kinetics of fluoride was studied in a batch condition. It was conducted by varying the adsorption time from 0 to 24 hours. The initial fluoride concentration was set at 10 - 25 mg/L in 250 mL of flasks with 5 g of BC in a phosphate buffer at pH 6.5 - 7.0. Then, the samples mixed with bone char were shaken at 200 rpm at room temperature. After the set time, they were filtered through a nylon syringe filter with a pore size of 0.45 µm to separate the water solutions and the BC adsorbents. The solutions were analyzed for their remaining fluoride concentration.

3.2.4.5 Adsorption isotherm study

The adsorption isotherm was studied by varying the initial concentration of fluoride from 1 to 16 mg/L in 50 mL of plastic bottle with 1 g of BC in the phosphate buffer at pH 6.5 - 7.0. The BC and sample mixture will be shaken at 200 rpm at room temperature. In addition, the equilibrium time of adsorption was based on the kinetic study results. After the equilibrium time, the samples were filtered through a nylon membrane filter with a pore size of 0.45 µm for

separating the water solutions and the BC adsorbents. The solutions were analyzed for their remaining fluoride concentrations.

3.2.5. Defluoridation process study

3.2.5.1 Examination of the fluoride removal capacity by bone char

Both synthetic and actual contaminated water samples were used to study the fluoride removal capacity by bone char in a batch condition. BC of 2 g was shaken with 100 mL of water sample at 200 rpm for the equilibrium time of each BC which was obtained from adsorption kinetic study. Then, the samples were filtered through a nylon membrane filter with a pore size of 0.45 μm for separating the solutions. The solutions were analyzed for their remaining fluoride concentrations. After that, the fluoride adsorption capacities in synthetic and actual contaminated water samples were calculated and compared.

3.2.5.2 Examination the factors influencing the fluoride adsorption process

3.2.5.2.1 Effect of pH of water sample

This step was examined by varying the initial pH of water sample from 4.0 to 12.0 using 0.1 N of nitric acid or 0.1 N of sodium hydroxide. In addition, the initial fluoride concentration was set at 10 – 25 mg/L. Then, BC of 2 g was shaken with 100 mL of water sample at 200 rpm until it reached to the equilibrium time. After that the samples were filtered through a nylon membrane filter with a pore size of 0.45 μm for separating the solutions. The solutions were analyzed for their remaining fluoride concentrations. Then, the fluoride adsorption capacities were calculated and compared.

3.2.5.2.2 Effect of initial concentration

This step was examined by varying the initial fluoride concentration from 10 to 100 mg/L. Then, BC of 2 g was shaken with 100 mL of water sample in a phosphate buffer at pH 6.5 - 7.0 at 200 rpm until it reached to the equilibrium time. After that the samples were filtered through a nylon membrane filter with a pore size of 0.45 μm for separating the solutions. The solutions were analyzed for their remaining fluoride concentrations. Then, the fluoride adsorption capacities were calculated and compared.

3.2.5.2.3 Effect of anion

- Effect of chloride ion

The water sample was prepared by varying the concentration of chloride ion at 10 – 50 mg/L by using NaCl and the initial fluoride concentration at 10 – 25 mg/L. Then, BC of 2 g was shaken with 100 mL of water sample at 200 rpm. After the equilibrium time, the samples were filtered through a nylon membrane filter with a pore size of 0.45 μm for separating the solutions. The solutions were analyzed for their remaining fluoride concentrations. Then, the fluoride adsorption capacities were calculated and compared.

- Effect of sulfate ion

The water sample was prepared by varying the concentration of sulfate at 10 – 50 mg/L by using Na_2SO_2 and the initial fluoride concentration at 10 – 25 mg/L. Then, BC of 2 g was shaken with 100 mL of water sample at 200 rpm. After the equilibrium time, the samples were filtered through a

nylon membrane filter with a pore size of 0.45 μm for separating the solutions. The solutions were analyzed for their remaining fluoride concentrations. Then, the fluoride adsorption capacities were calculated and compared.

3.2.5.3 Examination the desorption process of fluoride ion

This experiment started with adsorption process. BC of 2 g was shaken with 100 mL of water sample with the initial fluoride concentration of 10 -25 mg/L at 200 rpm. Next, the water for examining the desorption process was prepared by varying the pH of solution from 6.0 to 11.0 using 0.1 N of nitric acid or 0.1 N of sodium hydroxide. After the equilibrium time, the samples were filtered through a nylon membrane filter with a pore size of 0.45 μm for separating BC adsorbents and the solution. Then, the BC was added to 100 mL of water that was prepared for desorption process and shaken at 200 rpm for 6 hours. After that, the desorbed fluoride concentration was analyzed by measuring fluoride concentration in the aqueous phase.

3.2.6. Analytical method

3.2.6.1 Determination of fluoride ion

Fluoride ion concentration was determined according to the standard method 4500-F– D. SPADNS Method (1999). The first step was preparation the standard curve. The fluoride standard solution was prepared in the range of 0 – 1 mg/L by diluting to 50 mL with deionized water. Then, 10.00 mL of acid-zirconyl-SPADNS reagent were added in each standard and mixed well. The acid-zirconyl-SPADNS reagent was a mixture between a SPADNS solution (958 mg of SPADNS in 500 mL with deionized water) and zirconyl-acid reagent (133 mg of $ZrOCl_2 \cdot 8H_2O$ in 25 mL

of deionized water added with 350 mL HCl and diluted it to 500 mL with deionized water). The second step was preparation the water sample. Fifty mL of sample or diluted sample with less than 1 mg/L of F (to avoid F concentration beyond the range of standard curve) were prepared. Next, 10.00 mL of the acid-zirconyl-SPADNS reagent were added in the prepared sample and mixed well. Then, the absorbance of the mixture (or the standard) was analyzed by a UV-Spectrophotometer (UV-6400 SPECTROPHOTOMETER, JENWAY), 570 nm. In addition, a reference solution (10 mL of SPADNS solution to 50 mL of deionized water) was applied to reset the spectrophotometer prior to the absorbance measurement. Finally, the fluoride concentration (mg/L) in the sample was obtained from the standard curve which a plot between absorbance and F standard concentrations.

3.2.6.2 Determination of chloride ion

According to the standard method 4500-Cl– C. Mercuric Nitrate Method (1999), 100-mL sample or a smaller portion so that the chloride content is less than 10 mg were used. 1.0 mL of an indicator-acidifier reagent, which was prepared by dissolving, 250 mg s-diphenylcarbazone, 4.0 mL conc HNO_3, and 30 mg xylene cyanol FF in 100 mL 95% ethyl alcohol, was added in a sample. The color of the solution was green-blue at this step. It was light green color when the pH of solution was less than 2.0 and pure blue at pH of solution more than 3.8. Then, it was titrated with 0.0141 N of Hg $(NO_3)_2$ until the water sample turn to purple color which was the end point. Finally, the chloride concentration was calculated following equation 3.1.

$$\text{mg } Cl^-/L = \frac{(A-B) \times N \times 35.45}{mL\ of\ sample} \quad (3.1)$$

which *A* is mL titration for sample, *B* is mL titration for blank, and *N* is normality of $Hg(NO_3)_2$.

3.2.6.3 Determination of sulfate ion

Sulfate ion determination followed according to the standard method 4500-SO_4^{2-} E. Turbidimetric Method (1999). One hundred mL of sample or a suitable portion diluted to 100 mL were prepared in a 250-mL erlenmeyer flask. Then, 20 mL of a buffer B solution (30 g $MgCl_2 \cdot 6H_2O$, 5 g $CH_3COONa \cdot 3H_2O$, 1.0 g KNO_3, 0.111 g sodium sulfate, Na_2SO_4, and 20 mL acetic acid (99%) in 500 mL distilled water and make up to 1000 mL) were added to the sample and mixed it in a stirring apparatus. While stirring, $BaCl_2$ (0.3 - 0.4g) was added and timing began immediately. The sample was stir for 60 ± 2 s at a stable of speed. Then, the absorbance was measured at 5 ± 0.5 min by a UV-Spectrophotometer (UV-6400 SPECTROPHOTOMETER, JENWAY), 420 nm. After that the calibration curve was prepared in range of 200 to 1000 µg which was obtained from 2 – 10 mL of a standard sulfate solution. In addition, the absorbance of standard sulfate solutions was analyzed in the same manner as the sample. The amount of sulfate (µg) was obtained from the calibration curve which a plot between absorbance and sulfate standard concentrations. Finally, the sulfate concentration (mg/L) was calculated by following the equation 3.2.

$$\text{mg } SO_4^{2-}/\text{L} = \frac{\text{µg of sulfate}}{\text{volume of water sample}} \quad (3.2)$$

Table 3 The method and instrument for analyzing parameters

Instrument/Method	Parameter
UV-VIS method at 570 nm wavelength.	Initial fluoride concentration and Sulfate ion in form of Na_2SO_4
pH METER F-71	pH
Titration	Chloride ion in form of NaCl

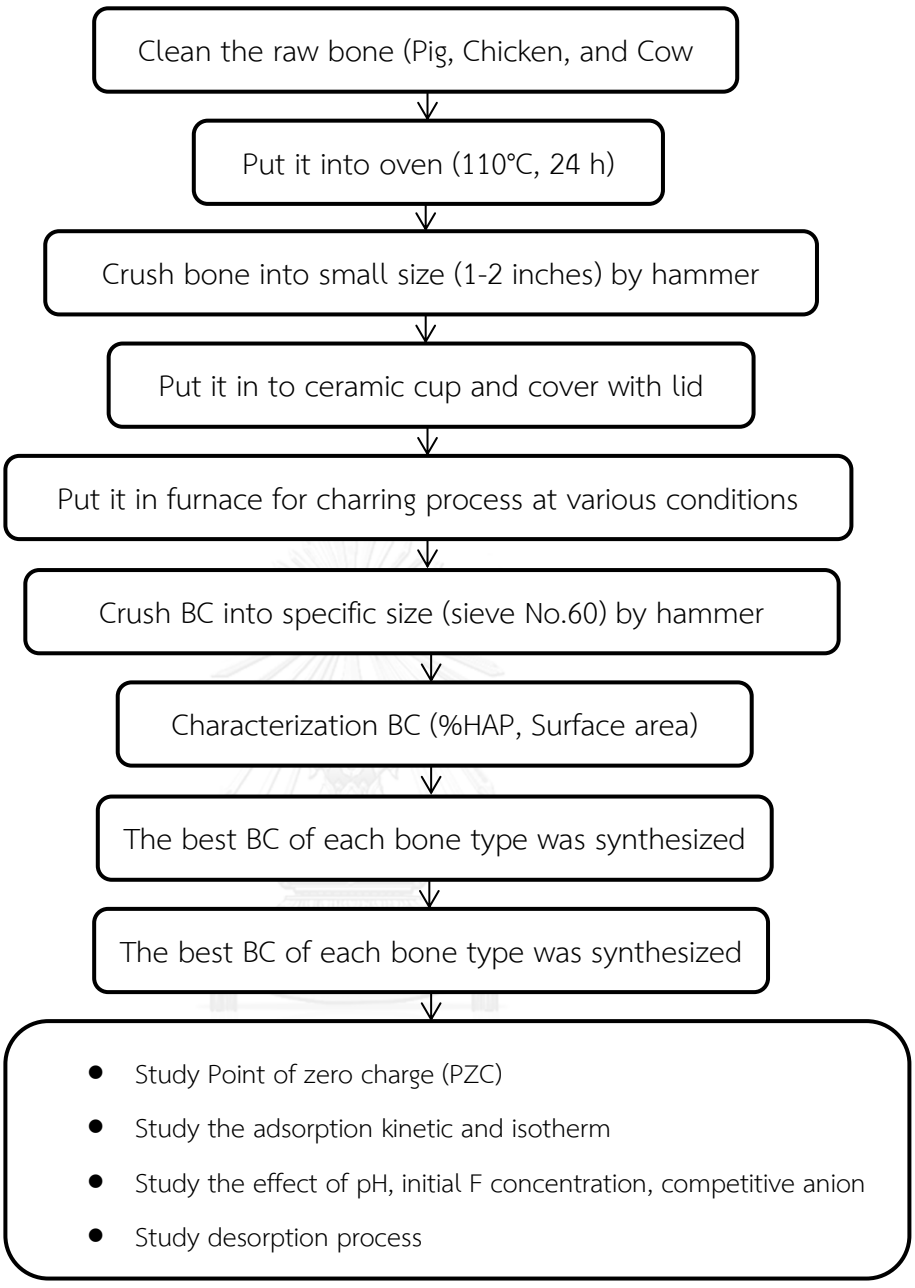

Figure 4 Summary of the step and methods for generating and characterizing BC adsorbents

CHAPTER 4

RESULTS AND DISCUSSION

4.1 BONE CHARS (BC) ADSORBENT CHARECTERISTIC

4.1.1 X-ray diffraction pattern

X-ray diffraction related results of synthesized pig BC (PBC), chicken BC (CKBC), and cow BC (CBC) adsorbents under 9 different conditions (charring temperatures at 450, 550, and 650°C with different duration time of 1, 2, and 3 hours) are illustrated in Figures 5 - 10. Figures 5 - 7 show the XRD pattern of hydroxyapatite (HAP) in PBC, CKBC, and CBC adsorbents. The charring condition at 650°C for 3 hours produced the highest amount of HAP in PBC and CKBC adsorbent. This condition generated the amount of HAP of PBC and CKBC adsorbents at 92.84% and 85.30% respectively. However, the highest amount of HAP in CBC was 63.13% at charring condition at 550°C for 3 hours. The higher amount of HAP was a result in the higher fluoride adsorption capacities.

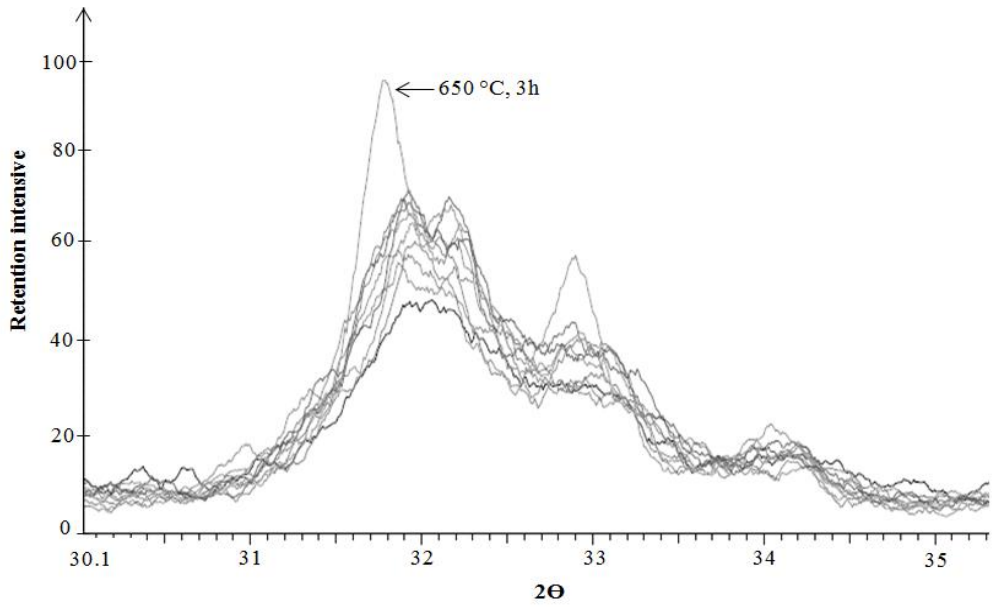

Figure 5 XRD pattern of PBC obtained at nine different pyrolysis conditions

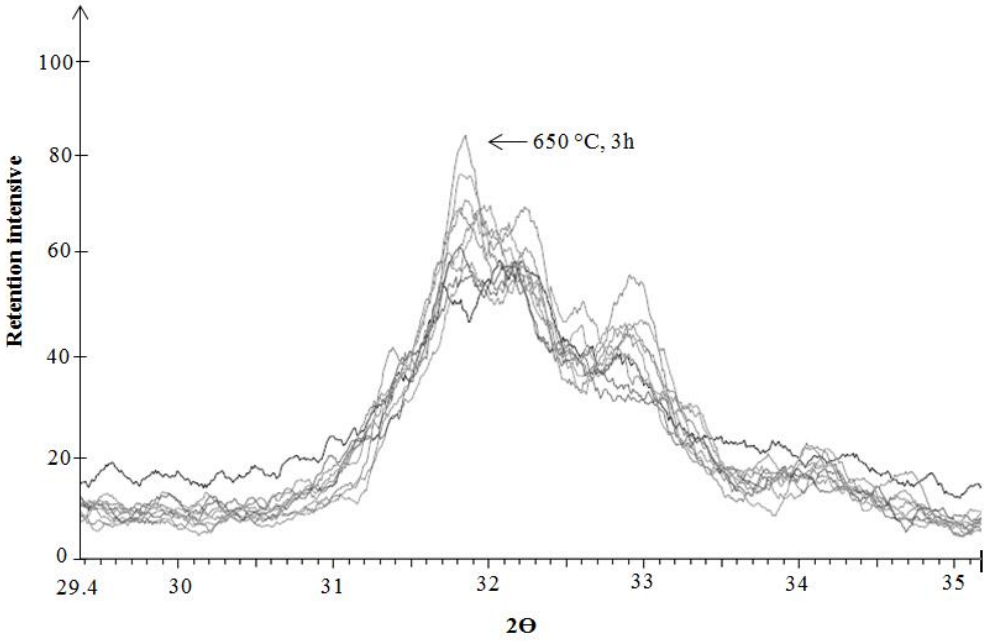

Figure 6 XRD pattern of CKBC obtained at nine different pyrolysis conditions

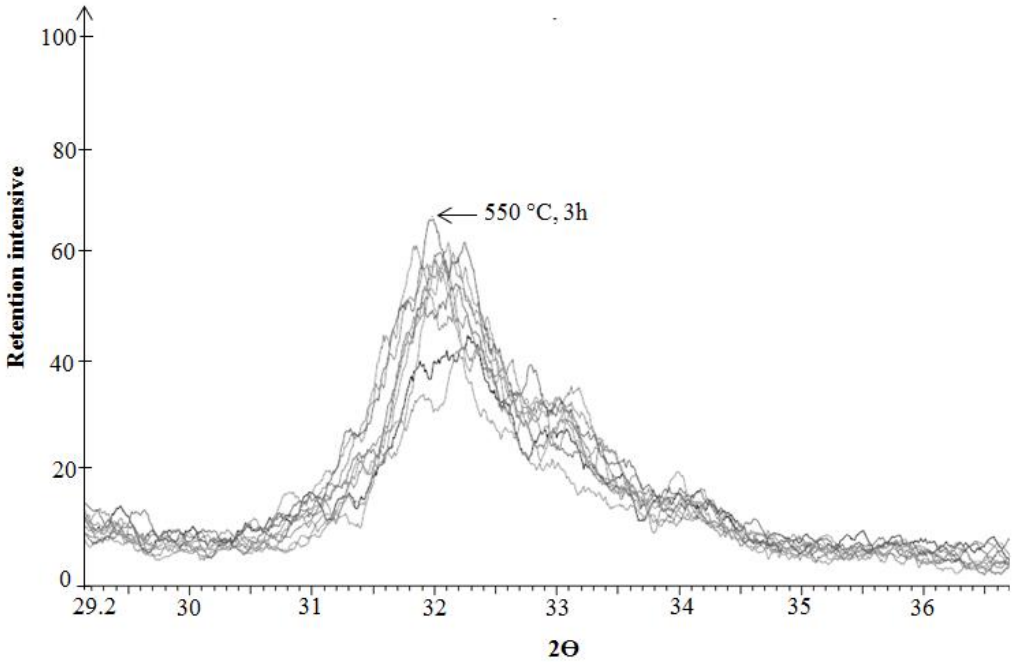

Figure 7 XRD pattern of CBC obtained at nine different pyrolysis conditions

The trend of HAP percentages at different charring conditions for PBC, CKBC, and CBC adsorbents was exhibited in Figures 8, 9, and, 10 respectively. The trend of HAP percentages in PBC and CKBC adsorbents gradually increased when the charring temperature was increased from 450°C to 650°C. The HAP percentage of CBC adsorbent tended to decrease when the charring temperature was increased from 550 °C to 650 °C. It is a result of the destruction of HAP at high charring temperature. Increasing charring duration also resulted in higher HAP percentage. For this study, the charring temperature lower than 450°C was not applied to avoid possible remaining some of organic matter on BCs. This generated condition can cause taste, odor, and/or color in treated water. In addition, the charring temperature higher than 650°C did not pursued because HAP could be destroyed at this temperature or higher (Rojas-Mayorga et al., 2013).

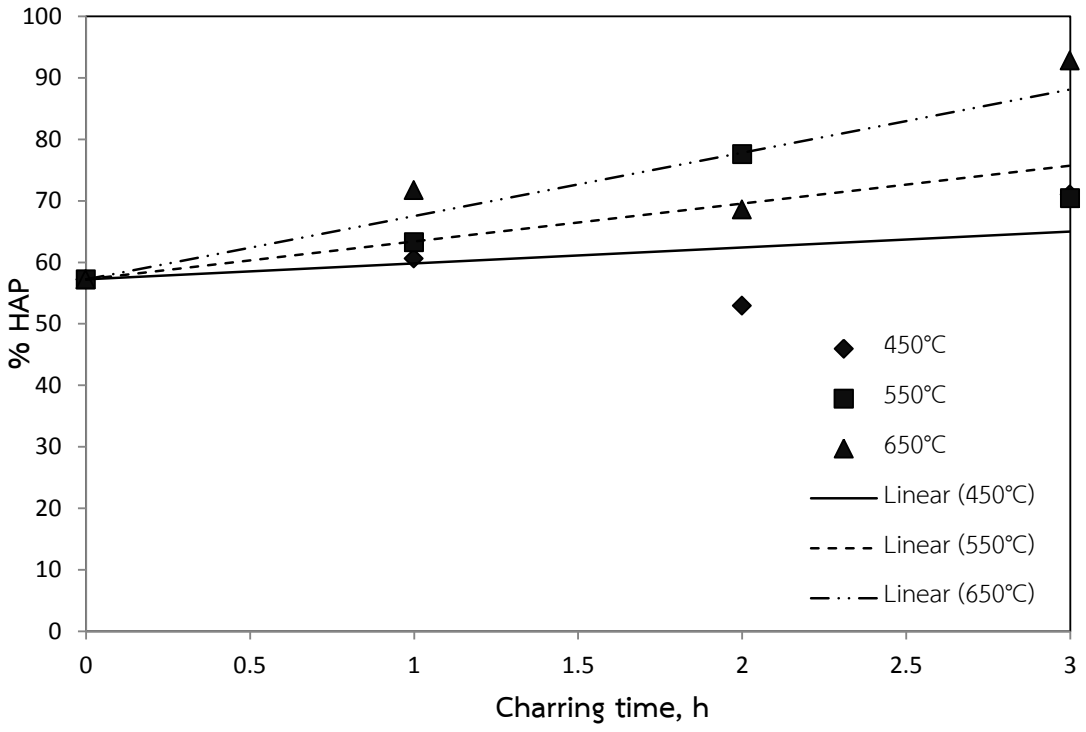

Figure 8 Relationship between charring time and %HAP in PBC for different charring temperature

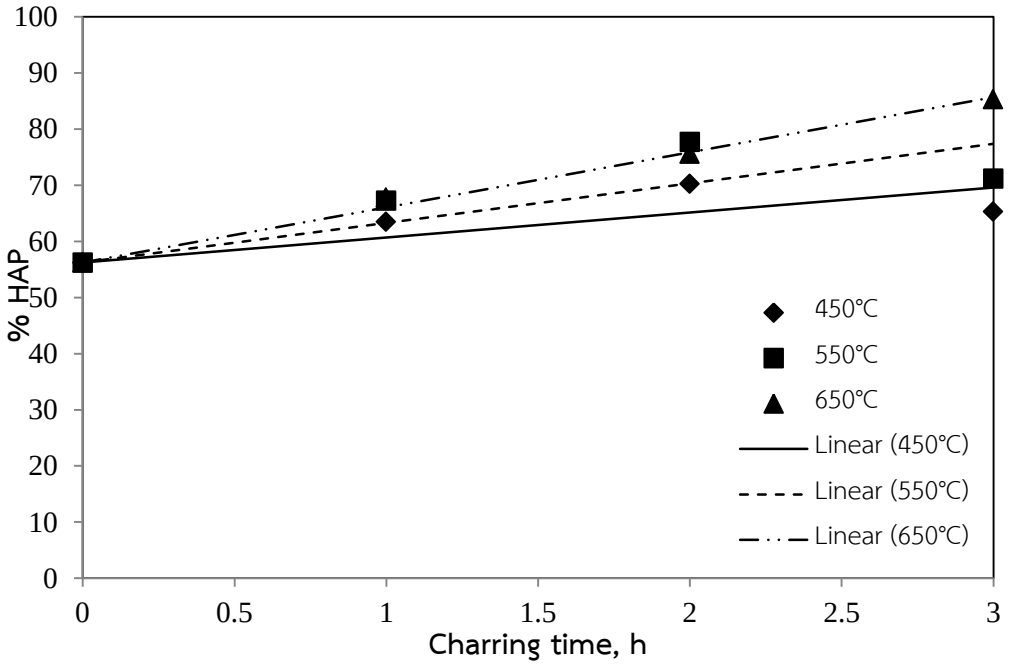

Figure 9 Relationship between charring time and %HAP in CKBC for different charring temperature

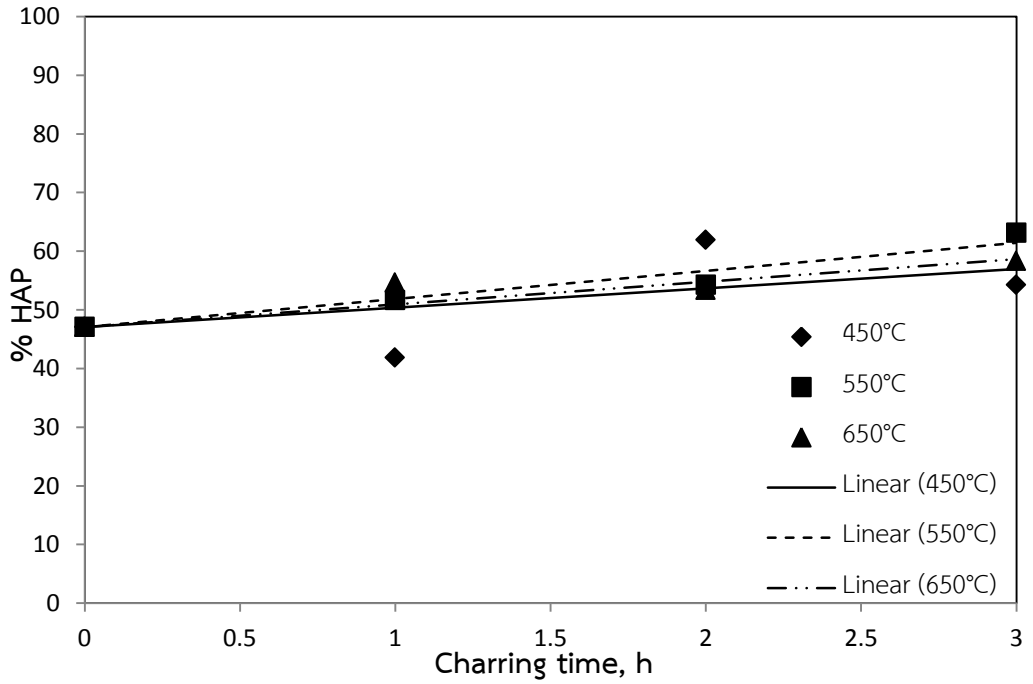

Figure 10 Relationship between charring time and %HAP in CBC for different charring temperature

4.1.2 Surface area and pore structure of PBC, CKBC and CBC adsorbents

The N_2 adsorption-desorption isotherms of PBC, CKBC, and CBC adsorbents are illustrated in Figures 11, 12, and 13, respectively. These isotherms and Brunauer-Emmett-Teller (BET) equation were used to calculate the surface area, pore volume, and average pore size of adsorbents. The values of these characteristics for PBC and CKBC charred at 650°C for 3 hours, and CBC charred at 550°C for 3 hours are shown in Table 4 respectively. CBC adsorbent had the highest specific surface area (103.11 m^3/g). In contrast, CKBC adsorbent had the lowest specific area when it was compared to other BC adsorbents. The specific surface area and pore volume are related to the fluoride adsorption capacity (Brunson & Sabatini, 2009). If adsorbents contained high specific area, the fluoride adsorption capacity also trend to be high. According to IUPAC classification (1985) (Figure 14), the N_2 adsorption-desorption isotherm of PBC and CKBC adsorbents were type II isotherm that was typical for nonporous materials with strong fluid-wall attractive forces. Furthermore, the N_2 adsorption-desorption isotherm of CBC were type IV that indicated mesoporous (pore width from 2 to 50 nm) with strong fluid-wall forces (Balbuenat & Gubbins, 1993).

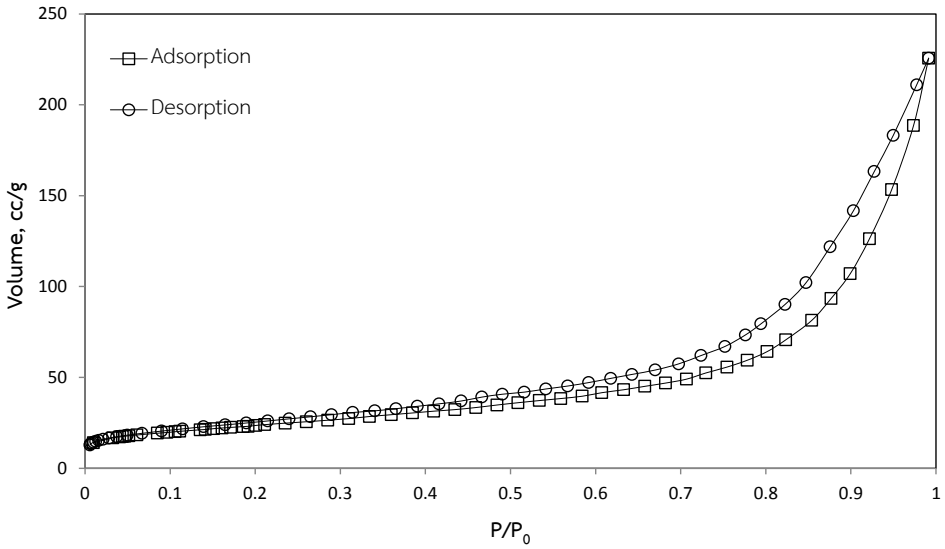

Figure 11 N_2 adsorption-desorption isotherms of PBC adsorbent

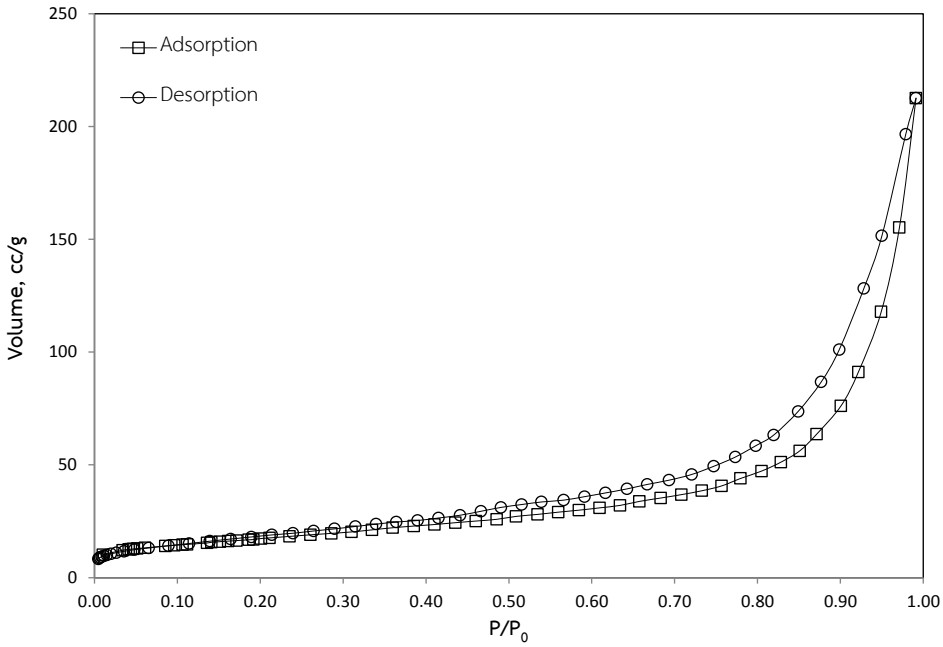

Figure 12 N_2 adsorption-desorption isotherms of CKBC adsorbent

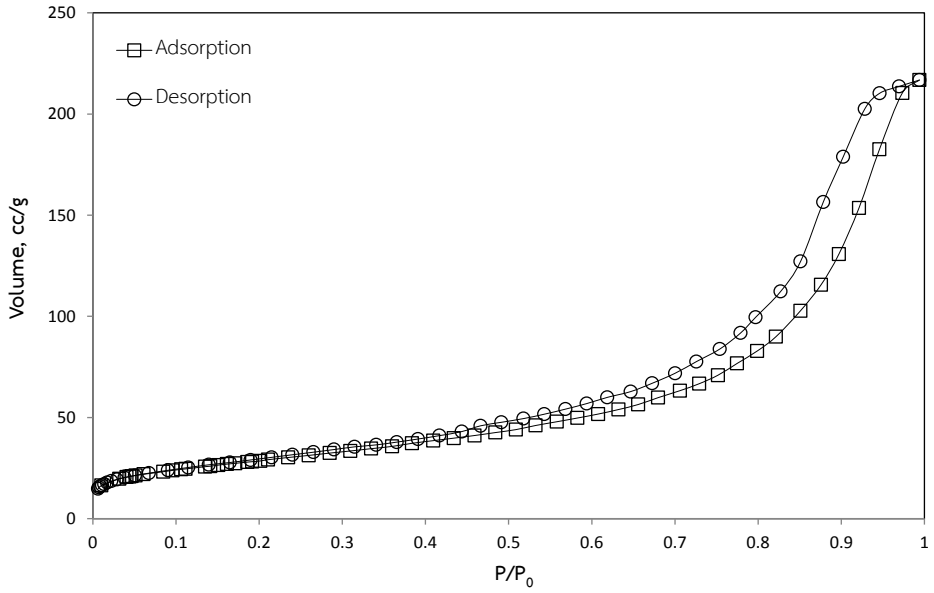

Figure 13 N_2 adsorption-desorption isotherms of CBC adsorbent

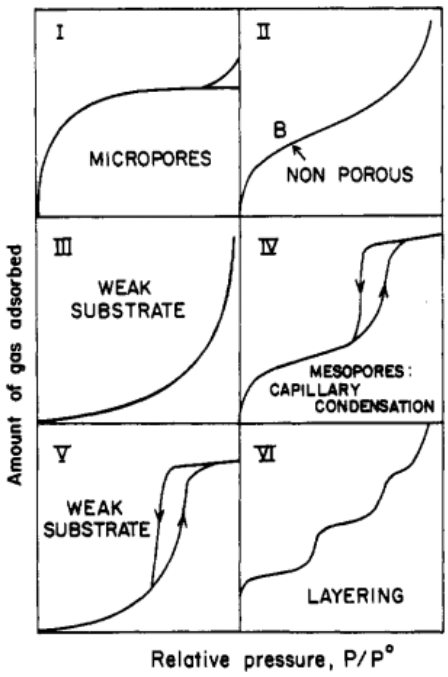

Figure 14 Types of adsorption isotherm, IUPAC classification (1985)

Table 4 BET surface area, pore volume, and average pore size of BC adsorbent

Parameter	PBC	CKBC	CBC
Specific surface area (m^2/g)	83.79	62.80	103.11
Total pore volume (cc/g)	0.3490	0.3288	0.3353
Average pore size (Å)	83.31	104.70	65.05

4.1.3 Surface charge density

The point of zero charge (PZC) values of synthesized PBC, CKBC, and CBC adsorbents were determined by considering the common plateau range of the plot of relationship as presented in Figures 15, 16 and 17, respectively. They were 8.6, 9.0 and 7.9 for PBC, CKBC, and CBC adsorbents, respectively. At pH equal to PZC, the surface change of adsorbents is neutral or nearly zero (Suaroon & Piyamongkala, 2012). Protonation reaction occurs at pH of solution lower than PZC value due to positive surface charge while the deprotonation took place when the surface of

adsorbents become negative because the pH solution is higher than the PZC value (Medellin-Castillo et al., 2014). In this study, the PBC, CKBC, and CBC adsorbents were applied to adsorb fluoride ion. Therefore, the positively charged surface of adsorbents was desired. As the positively charged condition condition, the pH of water sample was adjusted to pH range at 6.5 - 7.0 by adding phosphate buffer in this research.

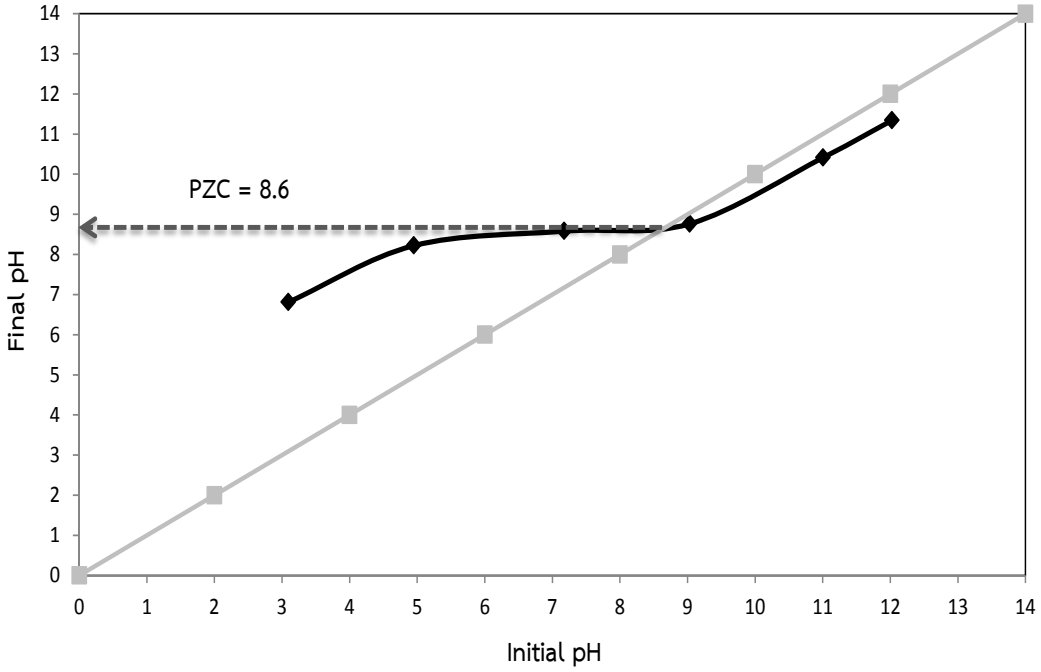

Figure 15 Determination of PZC of the PBC adsorbent

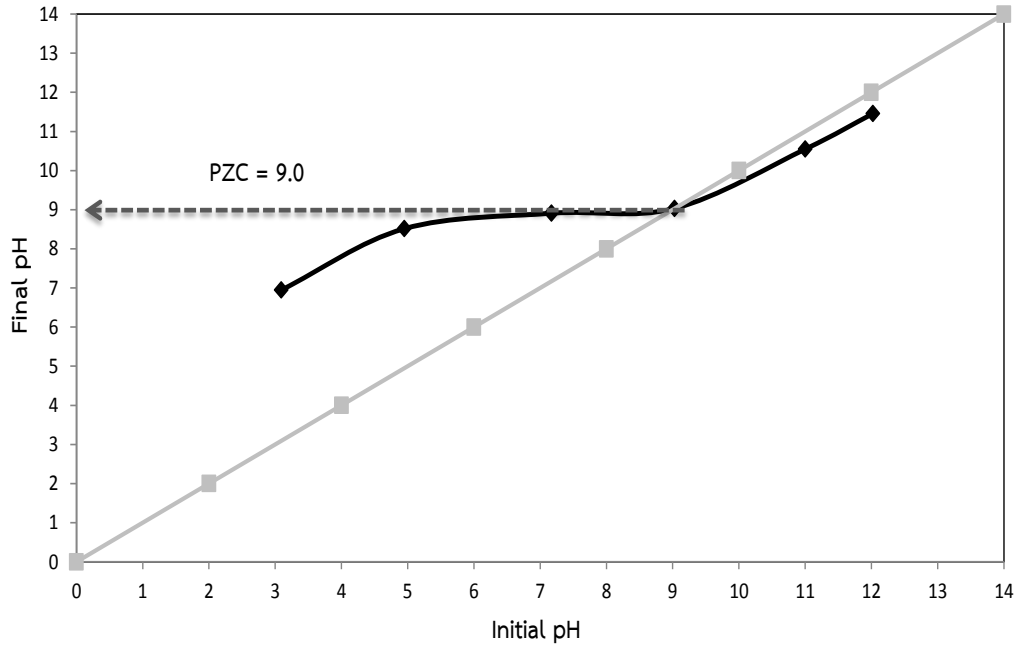

Figure 16 Determination of PZC of the CKBC adsorbent

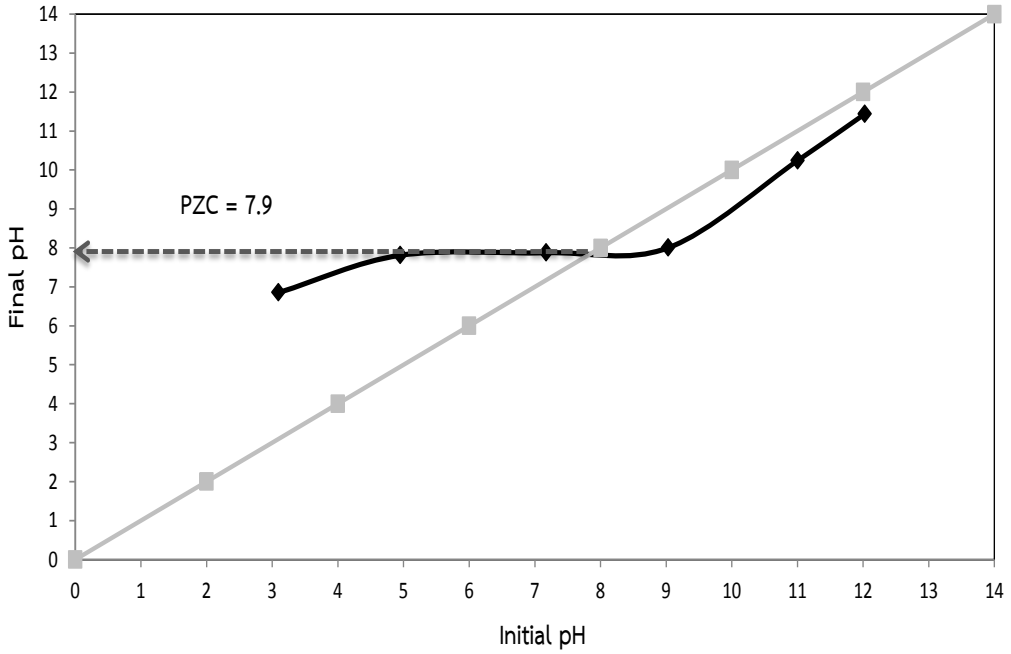

Figure 17 Determination of PZC of the CBC adsorbent

4.2 ADSORPTION OF FLUORIDE ION ON PBC, CKBC, and CBC

4.2.1 Adsorption kinetic

The kinetic curves of fluoride adsorption on PBC, CKBC, and CBC adsorbents are shown in Figure 18. All of the BC rapidly adsorbed fluoride ion in the first hour. After that, the adsorption was consistently slow until it reached equilibrium after 3 hours. The highest adsorption fluoride capacities on PBC, CKBC, and CBC adsorbents at equilibrium in experiment were 0.449, 0.337 and 0.527 mg/g, respectively. It was slightly higher than the fluoride adsorption capacities which were calculated from each kinetic model.

This study, the pseudo- first order and the pseudo- second order models were applied to the kinetics data in Figure 18 and the results are shown in Figures 19 and 20. The kinetic parameters summarized in Table 5. The R2 (the correlation coefficient) value was used to indicated the best fitting model of this study. Both models provided high R^2 values. However, the R^2 (the correlation coefficient) value of the pseudo-second order kinetic fit was higher than that of the pseudo-first order fit for all three types of BC adsorbents. Thus, it indicated that the pseudo-second order model was more suitable to describe the adsorption kinetics of fluoride ion on PBC, CKBC, and CBC adsorbents at a low initial fluoride concentration. The pseudo-second order kinetic reaction rate constants were 0.0996, 0.0576 and 0.0718 g/ (mg·min) for PBC, CKBC, and CBC adsorbents. The strong agreement between the pseudo-second order kinetics and the adsorption data suggests that chemisorption, which is an electrostatic interaction between fluoride ion and BC adsorbents, was dominating (Ho & Ofomaja, 2006). A previous study (Valencia-Leal, Cortés-Martínez, & Alfaro-Cuevas-Villanueva, 2012) found that the pseudo second order kinetic models is suitable describing fluoride biosorption kinetics.

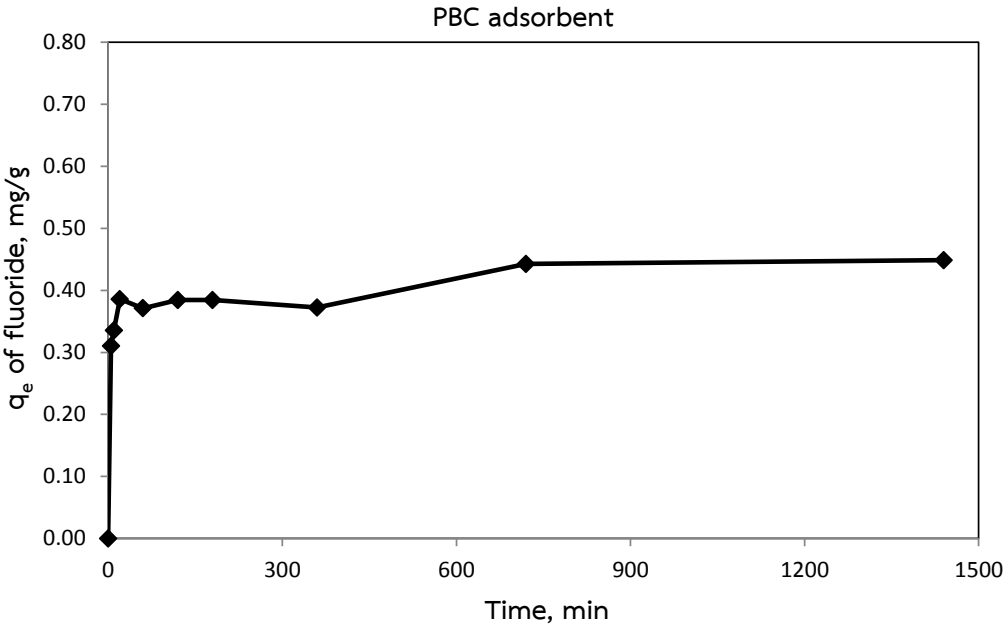
PBC adsorbent
0.80
0.70
0.60
0.50
0.40
0.30
0.20
0.10
0.00
q_e of fluoride, mg/g
0
300
600
900
1200
1500
Time, min

(a)

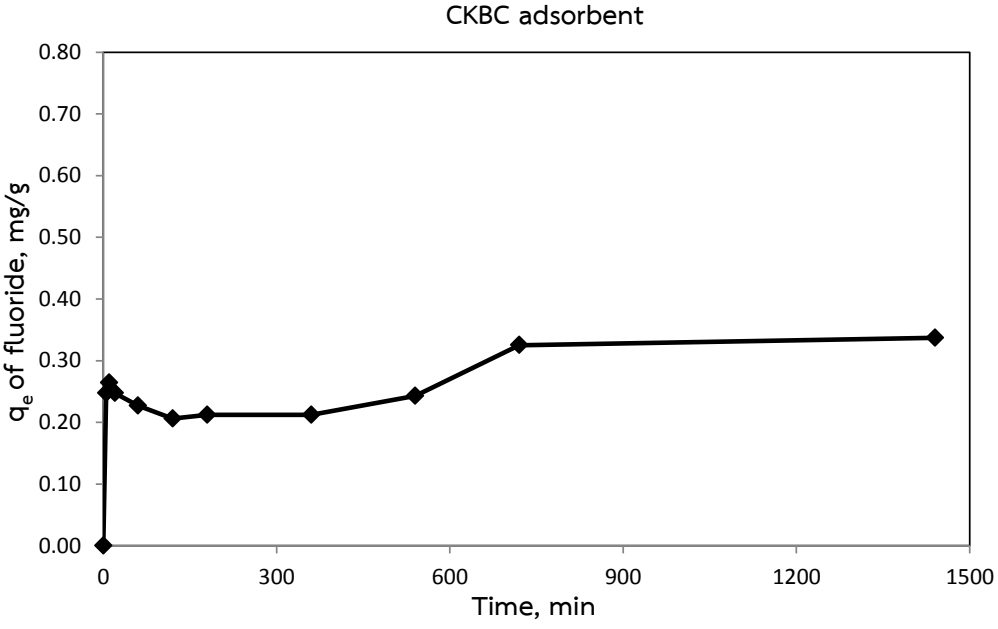
CKBC adsorbent
0.80
0.70
0.60
0.50
0.40
0.30
0.20
0.10
0.00
q_e of fluoride, mg/g
0
300
600
900
1200
1500
Time, min

(b)

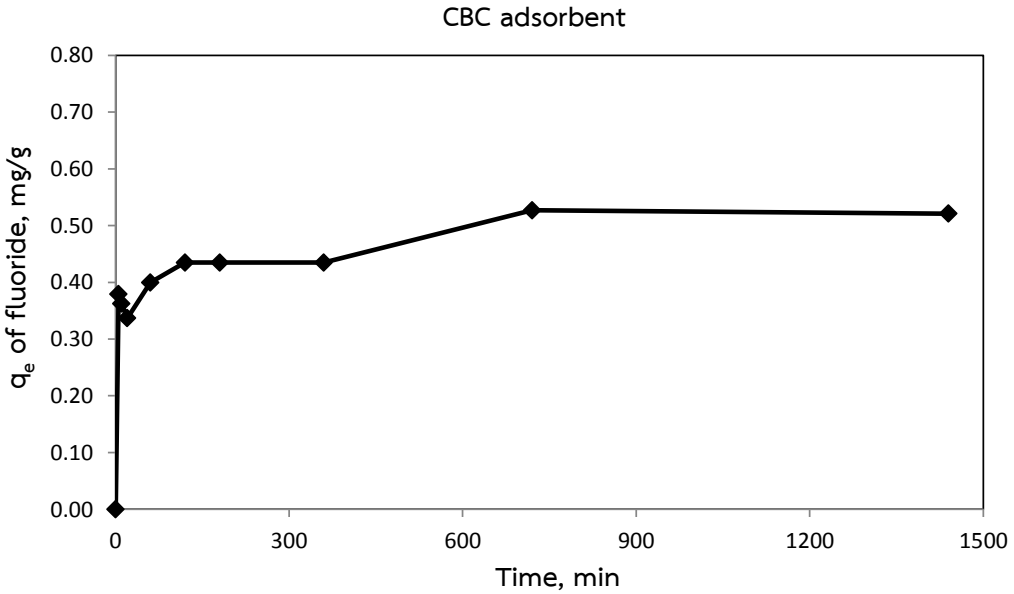

(c)

Figure 18 Kinetics adsorption of fluoride ion on (a) PBC, (b) CKBC, and (c) CBC

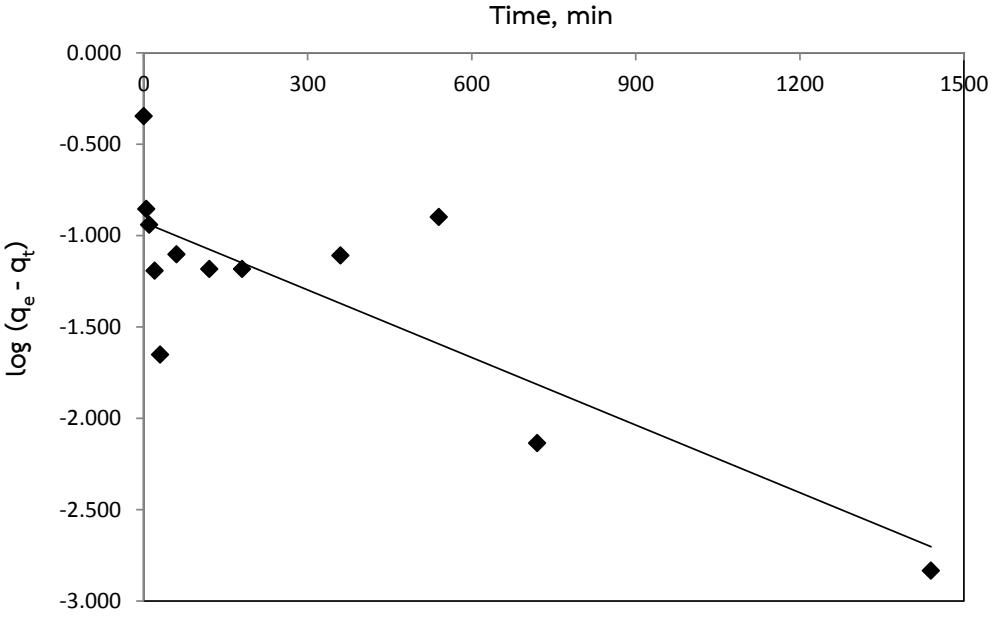

(a)

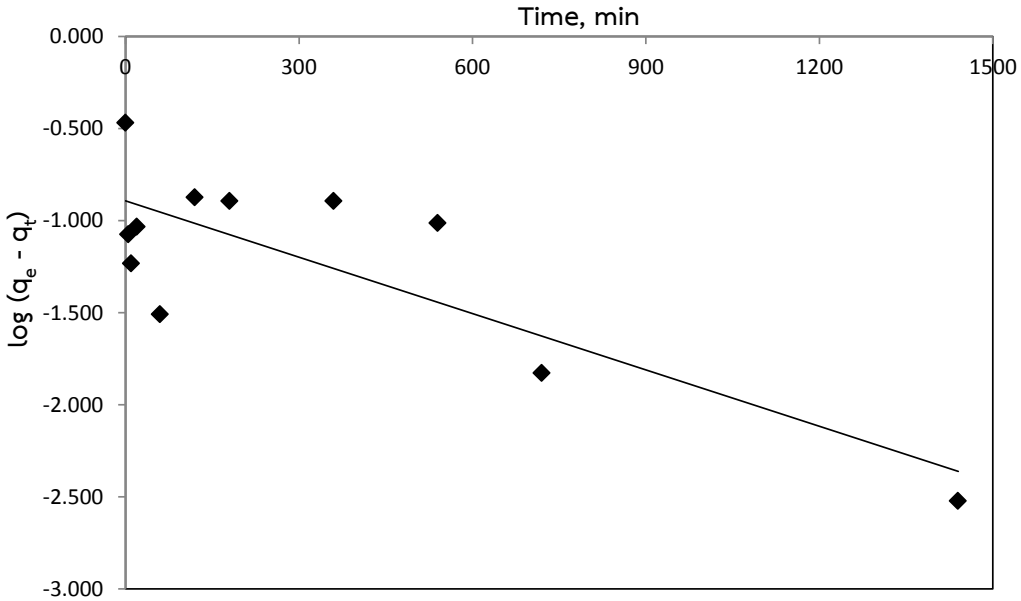

(b)

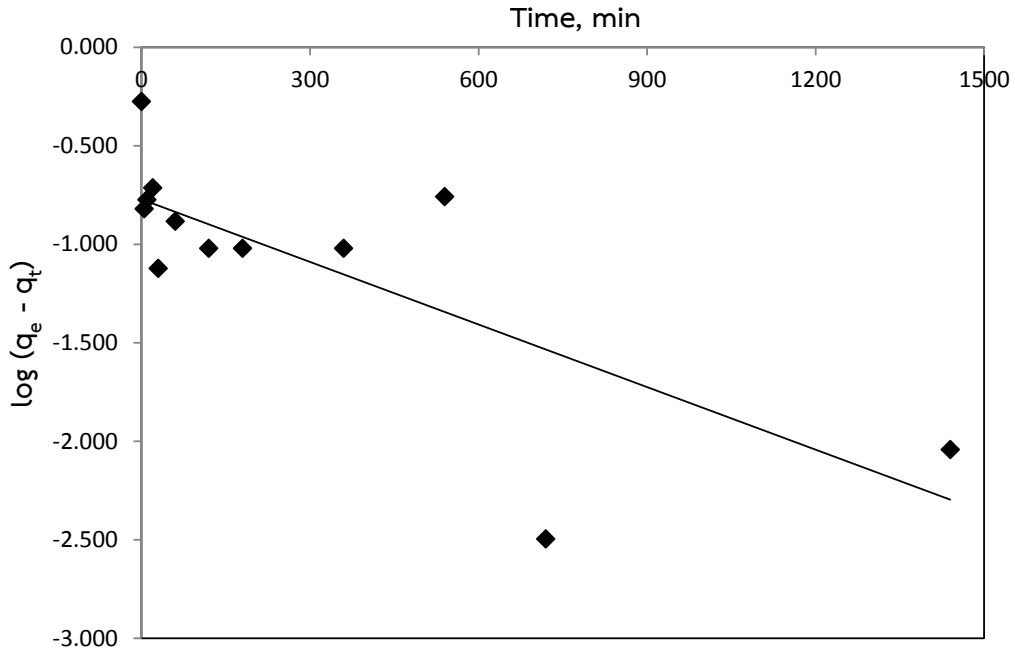

(c)

Figure 19 Pseudo-first order kinetic models for fluoride adsorption by (a) PBC (b) CKBC (c) CBC

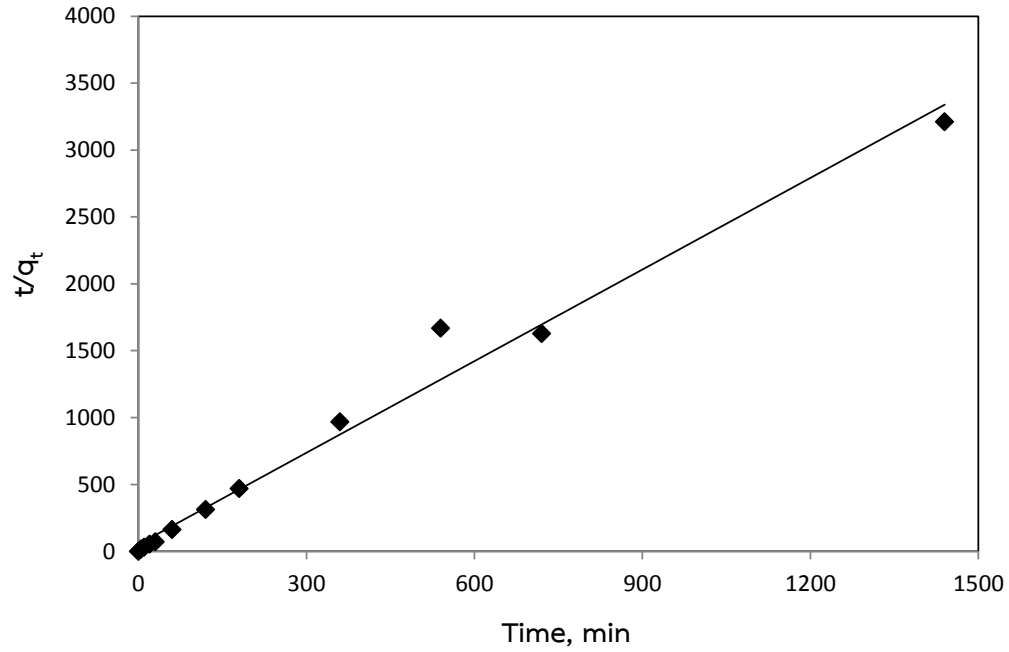
4000
3500
3000
2500
2000
1500
1000
500
0
t/qt
0
300
600
900
1200
1500
Time, min

(a)

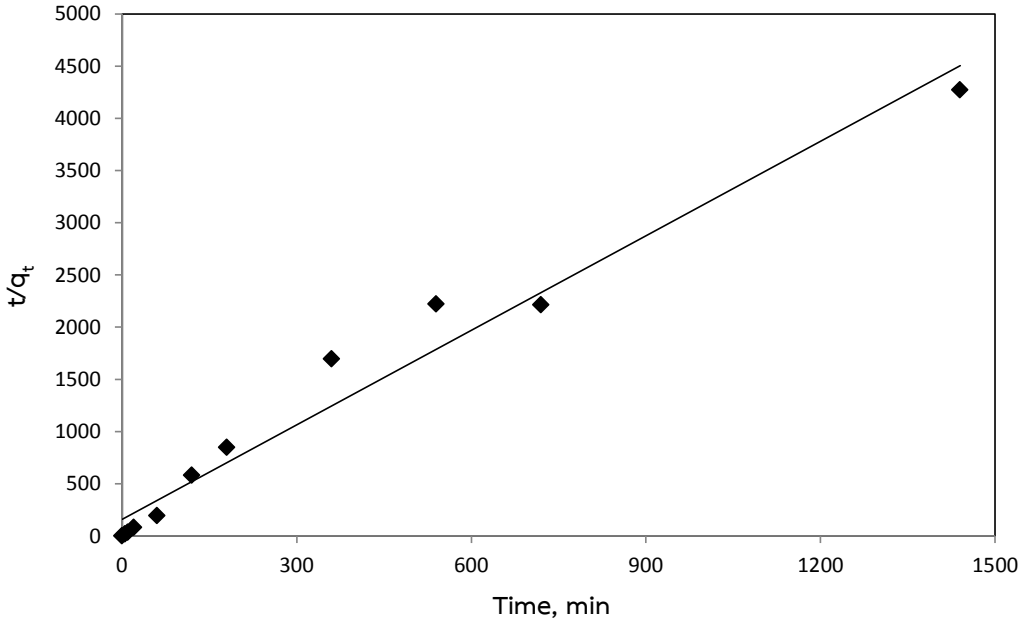
5000
4500
4000
3500
3000
2500
2000
1500
1000
500
0
t/qt
0
300
600
900
1200
1500
Time, min

(b)

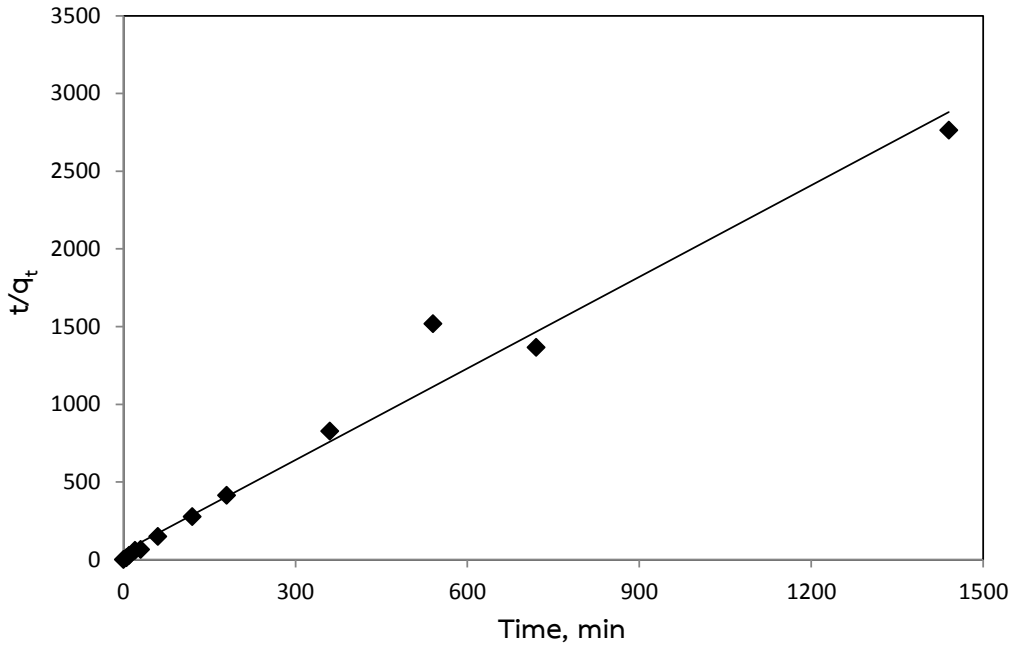

(c)

Figure 20 Pseudo-second order kinetic models for fluoride adsorption by (a) PBC (b) CKBC (c) CBC

Table 5 Kinetic parameters of fluoride adsorption on PBC, CKBC, and CBC adsorbents

Model	Parameter	PBC	CKBC	CBC
	$q_{e,exp}$ mg/g	0.449	0.337	0.527
Pseudo first order	R^2	0.6655	0.6566	0.571
	$q_{e,cal}$ mg/g	0.3952	0.41	0.462
	K_1, min^{-1}	0.0028	0.0023	0.0025
Pseudo second order	R^2	0.9826	0.9679	0.9749
	$q_{e,cal}$ mg/g	0.4382	0.3313	0.5095
	K_F, g/(mg·min)	0.0996	0.0576	0.0718

4.2.2 Adsorption isotherm model.

The fitting results of isotherm adsorption experimental data to Linear, Langmuir and Freundlich models are shown in Figures 21, 22 and 23, respectively and the fitting parameters are summarized in Table 6. The R^2 value of Langmuir isotherm model was the highest regardless of the BC type suggesting that the adsorption of fluoride ion on PBC, CKBC, and CBC adsorbents was monolayer. As this result, it was related to the result of surface area. CBC has the highest amount of surface area; it resulted in the highest fluoride adsorption capacity because the adsorption process occurred with monolayer. Other previous studies reported that the Langmuir sorption isotherm can be used to define the adsorption process of fluoride ion on BC material (Kashi, 2015; Mutchimadilok, Smittakorn, Mongkolnchai-arunya, & Durnford, 2014).

Besides, the linear isotherm model also best fits to the fluoride adsorption experimental results on all BC adsorbents because the equilibrium concentration of this experiment was low value that might be caused by setting at low initial fluoride concentration in this research. Thus, the linear isotherm model was also recommended in this study.

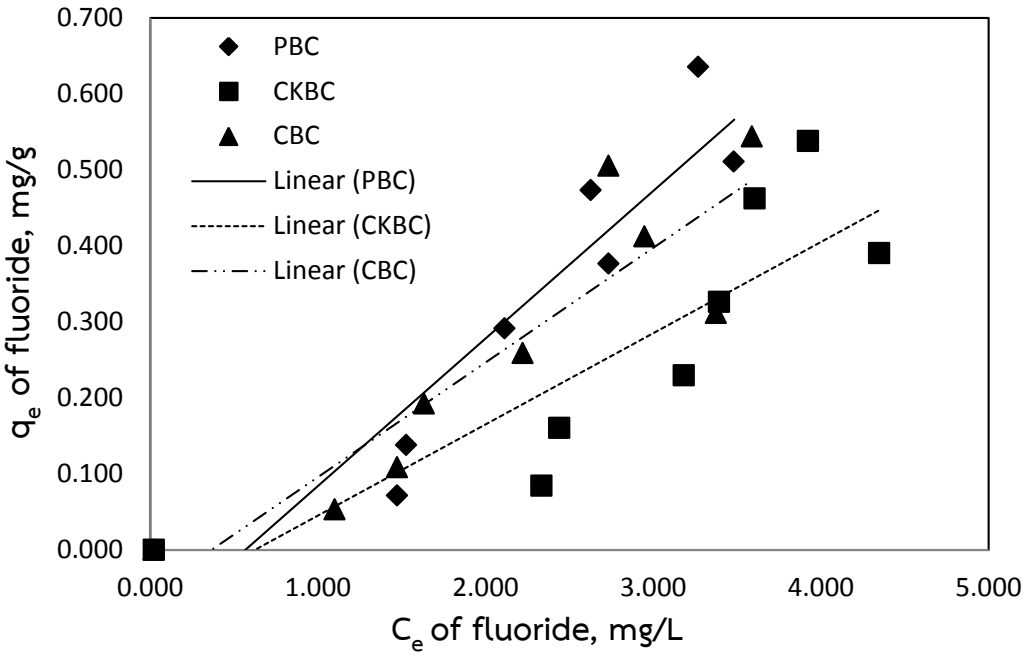

Figure 21 Fitting of adsorption data to linear isotherm model of PBC, CKBC, and CBC adsorbent

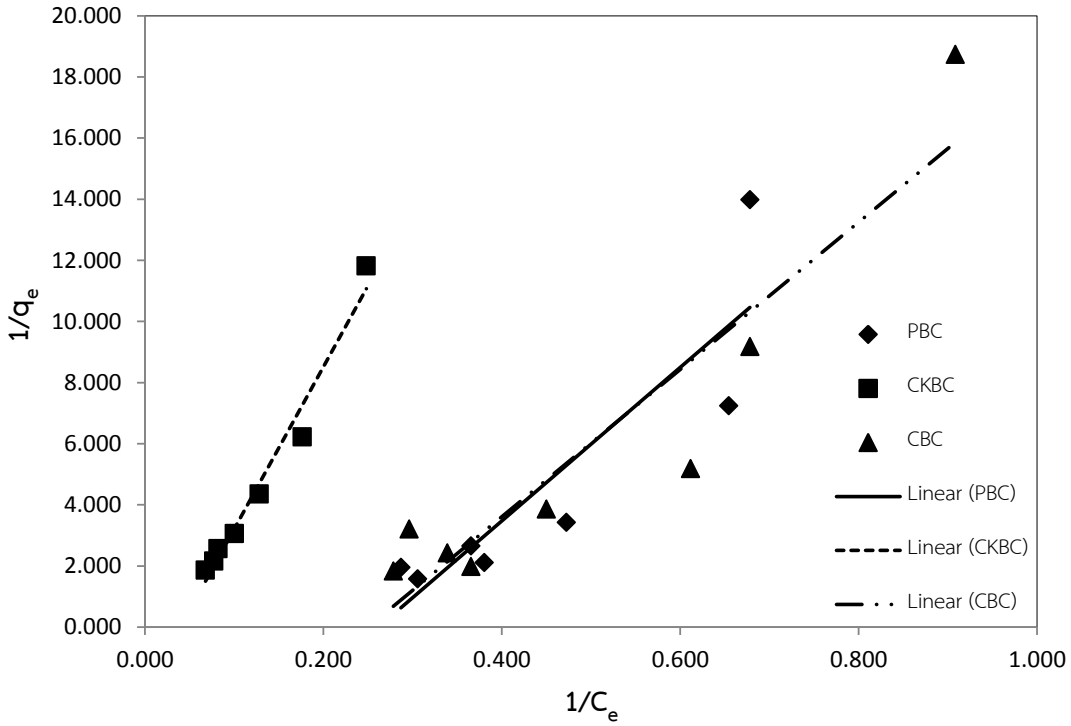

Figure 22 Fitting of adsorption data to Langmuir isotherm model of PBC, CKBC, and CBC adsorbents

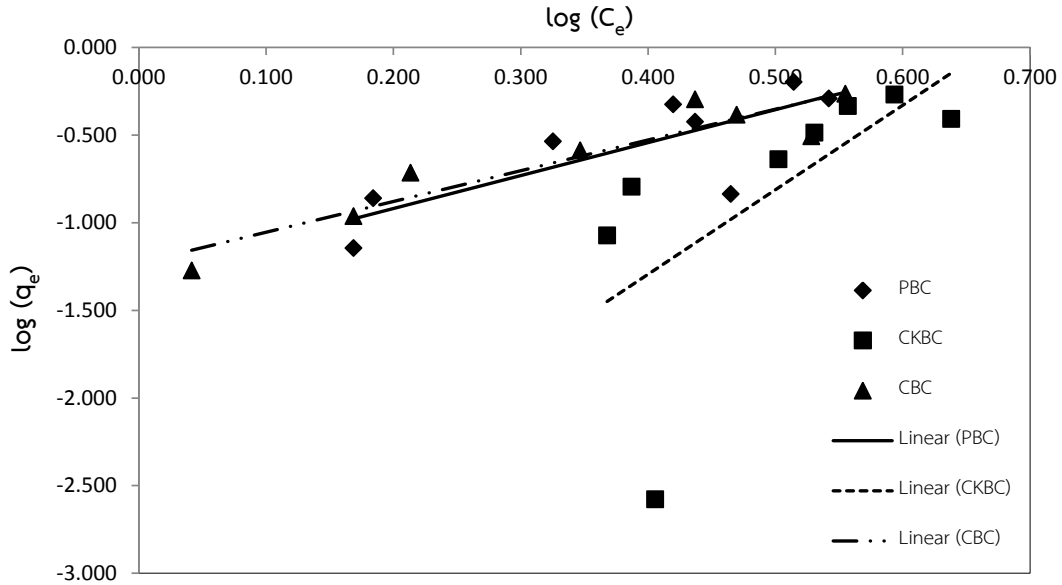

Figure 23 Fitting of adsorption data to Freundlich isotherm models of PBC, CKBC, and CBC adsorbents

Table 6 Isotherm parameters of the fluoride adsorption on the PBC, CKBC, and CBC adsorbents

Model	Parameter	PBC	CKBC	CBC
Linear	R^2	0.5210	0.6509	0.8161
	K_p, L/mg	0.0832	0.1256	0.1509
Langmuir	R^2	0.716	0.8949	0.9376
	q_m, mg/g	200	200	200
	K_L, L/mg	1.165×10^{-3}	1.264×10^{-4}	3.4×10^{-3}
Freundlich	R^2	0.4868	0.4127	0.8769
	n	1.3414	0.2073	0.5691
	K_F, L/g	0.5468	0.0398	0.2923

4.3 EFFECT OF pH OF SOLUTION ON FLUORIDE ADSORPTION

The relationship between fluoride adsorption capacity on PBC, CKBC, and PBC adsorbents and various initial pH solutions is shown in Figure 24. For adsorption on PBC adsorbent, the fluoride adsorption capacity was 0.134 mg/g when the pH of solution was at PZC value (PZC = 8.6). The fluoride adsorption capacity drastically decreased to 0.0367 - 0.079 mg/g when the pH of solution was higher than PZC value. On the contrary, it increased to 0.3660 mg/g when the pH of solution was lower than PZC.

For CKBC adsorbent, fluoride was adsorbed by 0.133 mg/g when the pH of solution was equivalent PZC value (PZC = 9.0). In addition, fluoride capacity was drastically decrease into 0.083 mg/g when the pH of solution higher than PZC value. However, the fluoride capacity was increasing to 0.152 mg/g when the pH of solution lowers than PZC value.

For CBC adsorbent, fluoride was adsorbed by 0.072 mg/g when the pH of solution was equivalent PZC value (PZC = 7.9). In addition, fluoride capacity was drastically decrease into 0.085 mg/g when the pH of solution higher than PZC value. However, the fluoride capacity was increasing to 0.187 mg/g when the pH of solution lowers than PZC value.

For this data, it can be concluded that the positively surface charge was occurred when the pH of solution was lower than PZC value. It related to the increasing adsorption fluoride capacity. In addition, it meant that the protonation reaction was the predominant reaction in this condition. On the other hand, the deprotonation reaction was occurred when the pH of solution higher than PZC value (Medellin-Castillo et al., 2014). The BC surface became negative charge when pH of solution was higher than PZC value resulting in decreasing fluoride adsorption capacity while it was positively charged when pH o solution was lower than PZC value. The results of this work resembled the reported result of Medellin-Castillo et

al. (2014). The mechanism of fluoride adsorption on BC was proven in this study. All of the BCs still adsorbed the fluoride at and below the PZC which corresponds to neutral and negative surface charge. This indicates that electrostatic interaction was not the only adsorption mechanism (Kashi, 2015); physisorption was also involved in the adsorption of fluoride ion on BCs.

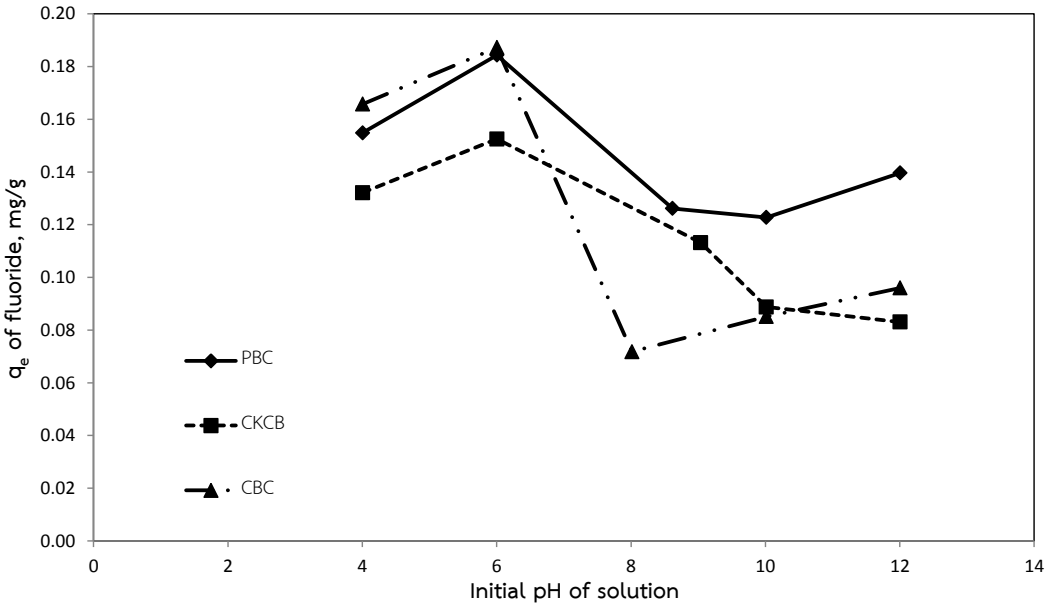

Figure 24 Effect of initial pH solution on Fluoride adsorption capacity on PBC, CKBC, and CBC adsorbents

4.4 EFFECT OF INITIAL FLUORIDE CONCENTRATION ON FLUORIDE ADSORPTION

The relationship between fluoride adsorption capacity and the increasing initial fluoride concentration was illustrated in Figure 25. The result shows that the increasing initial fluoride concentration from 13.941 to 83.024 mg/L resulted in the increasing adsorption fluoride capacity. It was related to the conceptual of linear isotherm model which occurred when the low initial fluoride concentration was set in this experiment. The fluoride adsorption capacities increased along with the increasing initial fluoride concentration. On the other hand, the adsorption fluoride

capacity slightly decreased when the initial fluoride concentration higher than 83.024 mg/L.

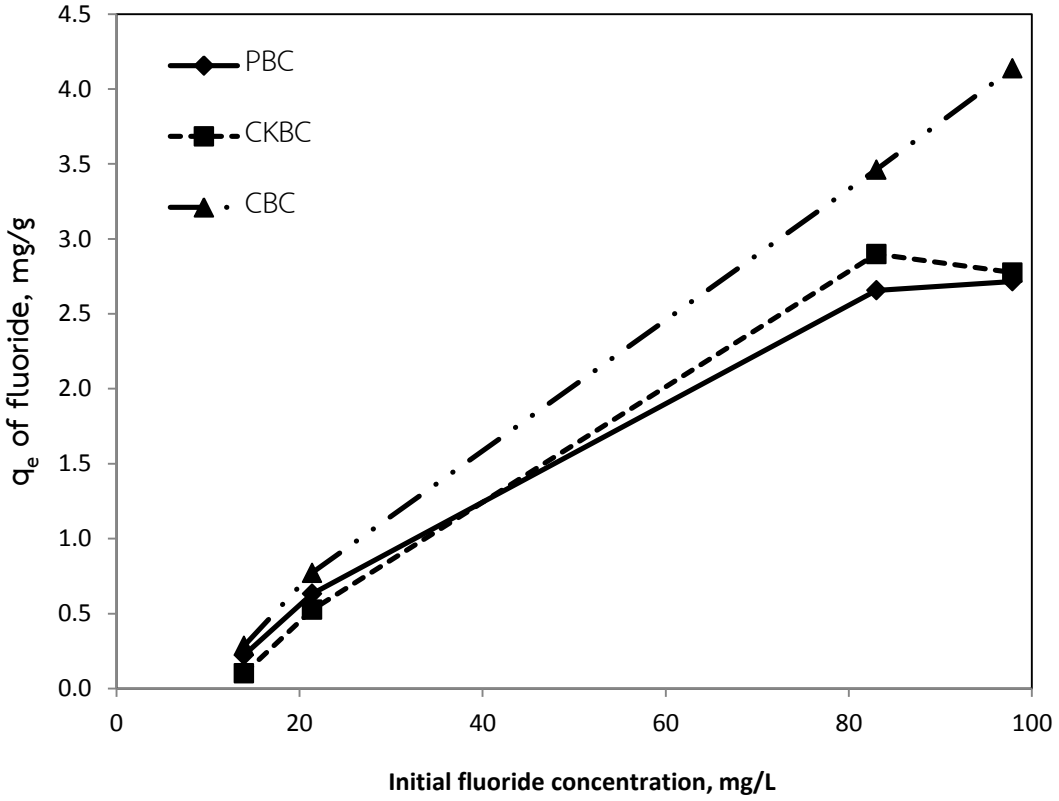

Figure 25 Effect of initial fluoride concentration on adsorption fluoride capacity on PBC, CKBC, and CBC adsorbents

4.5 EFFECT OF ANION ON FLUORIDE ADSORPTION

4.5.1 Effect of chloride

The relationship between the fluoride adsorption capacity on PBC, CKBC, CBC adsorbents and initial chloride concentration is illustrated in Figure 26. Initial chloride concentration had minimal effect on the fluoride adsorption capacity on PBC and CKBC adsorbents. On the other hand, the fluoride adsorption capacity on CBC adsorbent decreased from 0.557 to 0.281 mg/g with initial chloride concentration

increasing from 10 to 50 mg/L. It can be concluded that the initial chloride concentration affects the fluoride adsorption capacity of CBC adsorbent higher than those of PBC and CKBC adsorbents.

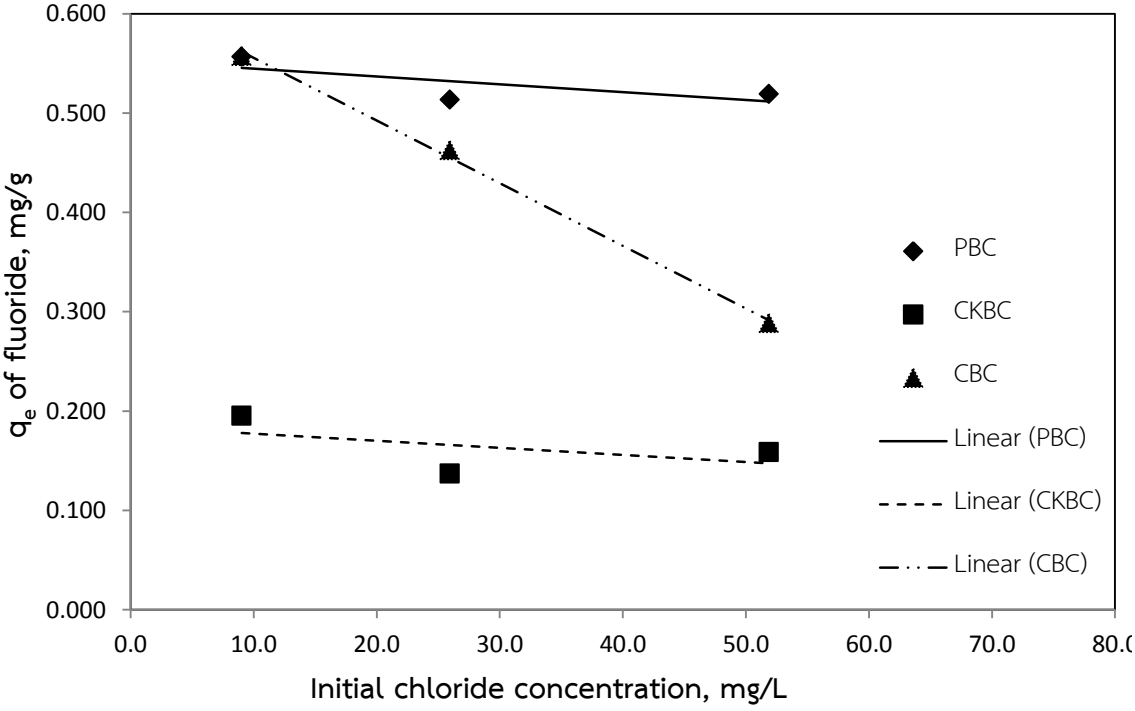

Figure 26 Effect of chloride ion on fluoride adsorption capacity on PBC, CKBC, and CBC adsorbents

4.5.2 Effect of sulfate ion

Figure 27 presents the relationship between fluoride adsorption capacity on PBC, CKBC, CBC adsorbents and initial sulfate concentration. The result shows that the increasing sulfate concentration decreased the fluoride adsorption capacity on PBC, CKBC, CBC adsorbents. However, the fluoride adsorption capacity on PBC adsorbents was slightly affected by increasing sulfate concentration the most.

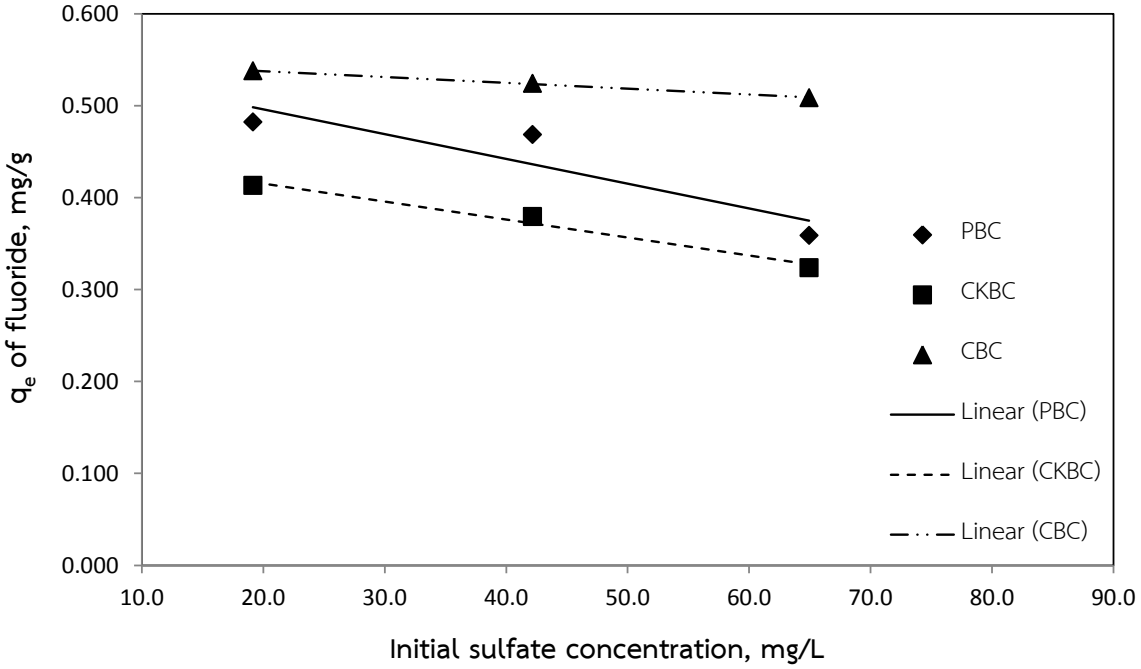

Figure 27 Effect of sulfate ion on fluoride adsorption capacity on PBC, CKBC, and CBC adsorbents

4.6 COMPARISON ADSORPTION FLUORIDE CAPACITIES ONTO BC ADSORBENTS FOR ACTUAL CONTAMINATED WATER FROM BAN BUAK KHANG SCHOOL AND SYNTHETIC WATER

The adsorption fluoride capacities onto PBC, CKBC, and CBC adsorbents for actual contaminated water and synthetic water were compared and summarized in Table 7. The result shows that for all 3 BC adsorbents, the fluoride adsorption capacity for the actual contaminated water was slightly higher than that of the synthetic water. The higher fluoride adsorption capacity associated with the actual contaminated water was due to other compositions from other constituents such as other anions and/or organic matter. It was able to react with fluoride ion as a result in increasing the fluoride adsorption capacity. Besides, the initial fluoride concentration of the actual contaminated water was higher than that of the synthetic

water. Consequently, the adsorption fluoride capacity was also higher. It related to the result of the study of effect of initial fluoride concentration in the work.

Table 7 Fluoride adsorption capacities, and initial and final fluoride ion concentration in contaminated and synthesized water samples

Parameter \ Type of BC		PBC	CKBC	CBC
Contaminated water sample	Initial concentration, mg/L	14.485	14.485	14.485
	Final concentration, mg/L	2.104	4.238	1.883
	q_e of fluoride, mg/g	0.617	0.489	0.628
Synthesized water sample	Initial concentration, mg/L	12.137	12.195	12.937
	Final concentration, mg/L	2.628	4.348	2.015
	q_e of fluoride, mg/g	0.474	0.390	0.542

4.7 DESORPTION PROCESS

Equilibrium fluoride adsorption onto PBC, CKBC, and CBC adsorbents was conducted and then the used BC adsorbents were soaked in deionized water at different pH value. Figure 28 illustrates the relationship between the fluoride adsorption capacity of each type and solution pH for desorption process from 6.0 to 11.0. The highest fluoride concentration was desorbed when pH solution higher than 11.0. However, at 6.0 and PZC value of pH solution for desorption process, the fluoride concentration still desorbed but it was minimal or no noticeable in water. Medellin-Castillo et al. (2014) observed similar result. They reported that fluoride

desorption when used cow bone char was loaded into an aqueous solution at pH 7.0 and 12.0

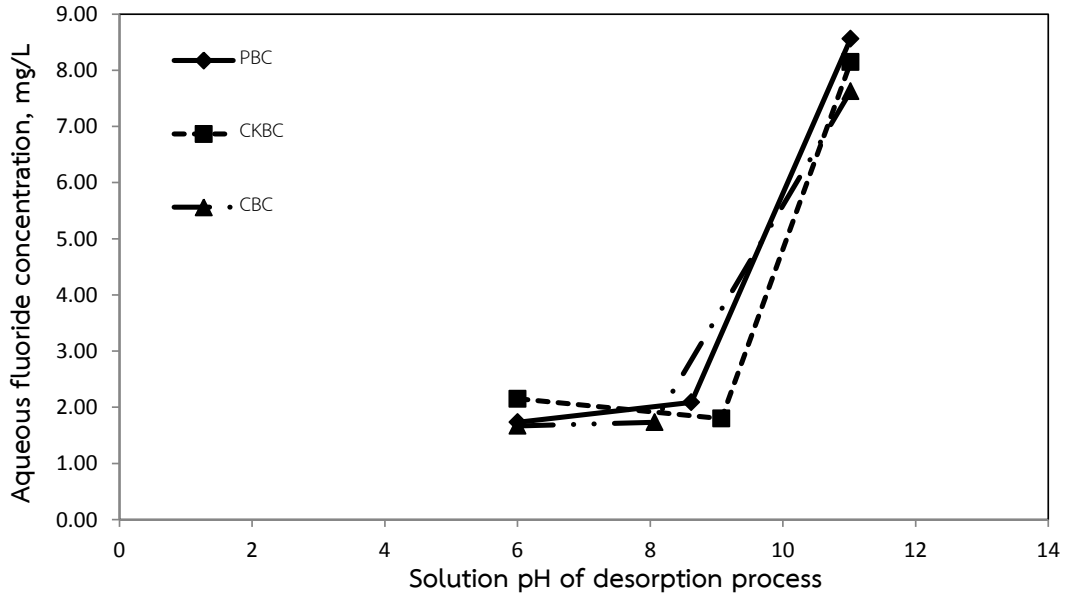

Figure 28 Effect of pH solution on fluoride desorption from PBC, CKBC, and CBC adsorbents

4.8 Total organic carbon analysis (TOC)

The results of amount of TOC, TC, and IC were summarized in Table 8. After both of synthetic water sample and actual contaminated water that contained fluoride ion were mixed with all BC adsorbents for adsorbing fluoride ion, the aqueous solution were examined the amount of TOC, TC, and IC in unit of mg/L. Firstly, all parameters contained in water sample at low concentration. After water samples were soaking with PBC, CKBC, and CBC adsorbents, the increasing of TOC, TC and IC concentration was occurred especially soaking with CBC adsorbent. It indicated that the fluoride ions were removed out but the other organics were released in treat water. As the result, the increasing of TOC releasing was a result in increasing initial fluoride ion of adsorption process by PBC, CKBC, and CBC adsorbents.

Table 8 Amount of TOC after adsorption process

Water sample	Type of BC in aqueous solution	TOC, mg/L	TC, mg/L	IC, mg/L
Actual contaminated water	-	2.355	27.51	25.15
	PBC	7.094	34.03	26.94
	CKBC	6.456	29.20	22.75
	CBC	17.64	38.81	21.16
Synthetic water at 10 mg/L of initial fluoride concentration	-	1.199	2.061	0.8626
	PBC	6.062	10.21	4.152
	CKBC	5.609	7.966	2.357
	CBC	22.31	25.14	2.830
Synthetic water at 50 mg/L of initial fluoride concentration	-	0.9378	1.412	0.4738
	PBC	7.249	11.46	4.211
	CKBC	6.258	7.857	1.599
	CBC	24.31	27.58	3.277

CHAPTER 5

CONCLUSIONS AND RECOMMENDATTIONS

5.1 CONCLUSIONS

The different type of bone applied the different charring condition for producing the best bone char adsorbents of each bone type. The best charring conditions for PBC and CKBC synthesis were 550°C for 3 hours and for CBC were 650°C for 3 hours. The charring temperature and time for PCB, CKBC, and CBC syntheses affected the amount of HAP generated. The highest amounts of HAP for PBC, CKBC, and CBC adsorbents were 92.8, 85.3 and 63.1%, respectively. It indicated that PBC contained the highest a percentage of HAP. However, CBC adsorbent had the highest amount of surface area. The points of zero charge of PBC, CKBC, and CBC adsorbents were 8.6, 9.0 and 7.9, respectively.

For the adsorption characteristics, fluoride adsorptions on PBC, CKBC, and CBC adsorbents reached the equilibrium after 3 hours of contact time. The adsorption agreed with the pseudo-second order kinetics with the rate constants of 0.0996, 0.0576 and 0.0718 g/ (mg·min), for PBC, CKBC, and CBC adsorbents, respectively. Furthermore, different BC adsorbents had different adsorption fluoride capacities. The highest fluoride adsorption capacities of PBC, CKBC, and CBC adsorbents were 0.449, 0.337 and 0.527 mg/g. Although the amount of HAP of CBC was lower than that of PBC, the fluoride adsorption capacity of CBC was higher than PBC. The fluoride adsorption capacity of BC is affected by not only the amount of HAP but also the surface area. In addition, fluoride adsorption onto BCs was monolayer as it followed the Langmuir isotherm model. The linear isotherm model also suitable for describing the fluoride adsorption on BCs at low initial fluoride concentration.

The pH of solution and anions affected to the adsorption fluoride capacity. At pH higher than the PZC, the adsorption fluoride capacity dramatically decreased increased because of negatively surface charge of BC adsorbents. In addition, it was negatively affected by chloride and sulfate ions in water. Low fluoride adsorption capacity was observed when synthetic contaminated water was used. The fluoride ions adsorbed on BC desorbed in water at pH higher than 11.0. The electrostatic interaction between BC surface and fluoride ion was dominant removal mechanism while physical interactions also contributed to the removal.

5.2 RECOMMENDATIONS AND FUTURE WORK

As results, all of three bone chars (PBC, CKBC, and CBC adsorbents) can be alternative material for fluoride removal in aqueous solution. Although CBC obtained the highest of fluoride adsorption capacity, the treat water still yellowish color. Thus, if CBC adsorbent was selected to apply in the actual contaminated water, the color improving process should be investigated. As a result of desorption process, the study of regeneration process and reuse efficiency of BCs adsorbent will be examined in further study. In addition, this work conducted all experiment under batch condition so the large scale of batch such as mixing tank will be designed for utilizing in the real situation in the future. Furthermore, the further study will be investigated the method for enhancing the surface area and amount of hydroxyapatite in order to increasing fluoride adsorption capacity. Finally, cost-benefit analysis will be conducted for comparing with the commercial adsorbents such as reverse osmosis membrane.

REFERENCES

Babic´, B. M., Milonjic´, S. K., Polovina, M. J., & Kaludierovic, B. V. (1999). Point of zero charge and intrinsic equilibrium constants of activated carbon cloth. *Carbon, 37*, 477–481.

Balbuenat, B. P., & Gubbins, E. K. (1993). Theoretical Interpretation of Adsorption Behavior of Simple Fluids in Slit Pores. *Langmuir, 9*, 1801-1814.

Ben Nasr, A., Walha, K., Charcosset, C., & Ben Amar, R. (2011). Removal of fluoride ions using cuttlefish bones. *Journal of Fluorine Chemistry, 132*(1), 57-62. doi:10.1016/j.jfluchem.2010.11.006

Bhatnagar, A., Kumar, E., & Sillanpää, M. (2011). Fluoride removal from water by adsorption—A review. *Chemical Engineering Journal, 171*(3), 811-840. doi:10.1016/j.cej.2011.05.028

Brunson, L. R., & Sabatini, A. D. (2009). An Evaluation of Fish Bone Char as an Appropriate Arsenic and Fluoride Removal Technology for Emerging Regions. *ENVIRONMENTAL ENGINEERING SCIENCE, Volume 26*, 1777-1783

Cai, H.-m., Chen, G.-j., Peng, C.-y., Zhang, Z.-z., Dong, Y.-y., Shang, G.-z., . . . Wan, X.-c. (2015). Removal of fluoride from drinking water using tea waste loaded with Al/Fe oxides: A novel, safe and efficient biosorbent. *Applied Surface Science, 328*, 34-44. doi:10.1016/j.apsusc.2014.11.164

Dahi, E., & Breghoj, H. (1995). Significance of oxygen in processing of bone char for defluoridation of water. *Proceedings of the 1st International Workshop on Fluorosis Prevention and Defluoridation of Water*, 96-103.

Ho, S. Y., & Ofomaja, E. A. (2006). Pseudo-second-order model for lead ion sorption from aqueous solutions onto palm kernel fiber. *J Hazard Mater, B129*, 137–142.

Jimenez-Reyes, M., & Solache-Rios, M. (2010). Sorption behavior of fluoride ions from aqueous solutions by hydroxyapatite. *J Hazard Mater, 180*(1-3), 297-302. doi:10.1016/j.jhazmat.2010.04.030

Kainosho, H., Wongrueng, A., Tokunaga, T., Takizawa, S., Hayashi, T., Wattanachira, S., & Mogi, K. (n.d.). The process controlling fluoride contamination in groundwater, Lamphun province, Thailand.

Kashi, G. (2015). Removal of Fluoride from Urbane Drinking Water by Bone Char *Journal of Chemical Engineering and Chemistry Research, 2*(7), 719-726.

Leyva-Ramos, R., Rivera-Utrilla, J., Medellin-Castillo, N. A., & Sanchez-Polo, M. (2010). Kinetic modeling of fluoride adsorption from aqueous solution onto bone char. *Chemical Engineering Journal, 158*(3), 458-467. doi:10.1016/j.cej.2010.01.019

Loganathan, P., Vigneswaran, S., Kandasamy, J., & Naidu, R. (2013). Defluoridation of drinking water using adsorption processes. *J Hazard Mater, 248-249*, 1-19. doi:10.1016/j.jhazmat.2012.12.043

Medellin-Castillo, A. N., Leyva-Ramos, R., Padilla-Ortega, E., Ocampo Perez , R., Flores-Cano, J. V., & Berber-Mendoza, M. S. (2014). Adsorption capacity of bone char for removing fluoride from water solution. Role of hydroxyapatite content, adsorption mechanism and competing anions. *Journal of Industrial and Engineering Chemistry, 20*, 4014–4021.

Mohapatra, M., Anand, S., Mishra, B. K., Giles, D. E., & Singh, P. (2009). Review of fluoride removal from drinking water. *J Environ Manage, 91*(1), 67-77. doi:10.1016/j.jenvman.2009.08.015

Mutchimadilok, Y., Smittakorn, S., Mongkolnchai-arunya, S., & Durnford, D. (2014). Defluoridation with Locally Produced Thai Bone Char. *Advances in Environmental Chemistry, Volume 2014* Article ID 483609.

Patel, S., Han, J., Qiu, W., & Gao, W. (2015). Synthesis and characterisation of mesoporous bone char obtained by pyrolysis of animal bones, for environmental application. *Journal of Environmental Chemical Engineering, 3*(4), 2368-2377. doi:10.1016/j.jece.2015.07.031

Piyamungkala, K., Talwat, J., Phothimongkonkul, P., & Kongsompak, C. (2008). Kinetic Adsorption of Chromium (VI) from Electroplating Factory onto Chitosan Resin. *The Journal of KMUTNB, Vol. 18*, No. 1.

Rao, S. M., Reddy, B. V., Lakshmikanth, S., & Ambika, N. S. (2009). Re-use of fluoride contaminated bone char sludge in concrete. *J Hazard Mater, 166*(2-3), 751-756. doi:10.1016/j.jhazmat.2008.11.115

Rojas-Mayorga, C. K., Bonilla-Petriciolet, A., Aguayo-Villarreal, I. A., Hernández-Montoya, V., Moreno-Virgen, M. R., Tovar-Gómez, R., & Montes-Morán, M. A. (2013). Optimization of pyrolysis conditions and adsorption properties of bone char for fluoride removal from water. *Journal of Analytical and Applied Pyrolysis, 104*, 10-18. doi:10.1016/j.jaap.2013.09.018

Singh, J., Singh, P., & Singh, A. (, 2014). Fluoride ions vs removal technologies: A study. *Arabian Journal of Chemistry*. doi:10.1016/j.arabjc.2014.06.005

Srimurali, M., Pragathi, A., & Karthikeyan, J. (1998). A study on removal of fluorides from drinking water by adsorption onto low-cost materials. *ENVIRONMENTAL POLLUTION, 99*, 285-289.

Suaroon, K., & Piyamongkala, K. (2012). Kinetic Adsorption of Silver Ion by Chitosan Resin. *KKU Sci. J., 40*, 1285-1300.

Thailand, T. M. o. P. H. o. (2002). Water quailty standard for drinking water. Retrieved from http://plan.dgr.go.th/school/5.pdf

Tor, A. (2006). Removal of fluoride from an aqueous solution by using montmorillonite. *Desalination, 201*(1-3), 267-276. doi:10.1016/j.desal.2006.06.003

Valencia-Leal, A. S., Cortés-Martínez, R., & Alfaro-Cuevas-Villanueva, R. (2012). Evaluation of Guava Seeds (Psidium Guajava) As a LowCost Biosorbent for the Removal of Fluoride from Aqueous Solutions. *International Journal of Engineering Research and Development, 5*(4), 69-76.

Wongrueng, A., Takizawa, S., Matsui, Y., Oguma, K., & Wattanachira, S. (Received May 23, 2008). Analysis of ULPRO membrane fouling used for groundwater defluoridation.

Wongruwng, A., Sookwong, B., Rakruam, P., & Wattanachira, S. (accepted 2015). Kinetic adsorption of Fluoride from Aqueous Solution onto Dolomite Sorbent

WorldHealthOrganization. (2006). Fluoride in drinking-water. Retrieved from http://www.who.int/water_sanitation_health/publications/fluoride_drinking_water_full.pdf

APPENDIX

APPENDIX A

ADSORBENT SYNTHESIS CHARACTERIZATIONS, EXPERIMENTS

1. Method for generating PBC, CKBC, and CBC adsorbents

1.1 Preparing and cleaning raw bones (pig, chicken, cow bones)

a1. **b1.** **c1.**

* a1. pig bone, b1. chicken bone, and c1. cow bone

1.2 Eliminating moisture by putting in an oven (100 ℃ for 24 hours).

1.3 Drying bones

a2. **b2.** **c2.**

* a2. pig bone, b2. chicken bone, and c2. cow bone

1.4 Crushing dry bone was into small pieces (1-2 inches) by machine or hammer

1.5 Tranferring crushed bones into ceramic cups and covering with lids

1.6 Charring by putting ceramic cups in a furnace under various conditions

1.7 Bone chars

1.8 Crushing BC into a specific adsorbent size (sieve size 600 µm)

1.9 Cleaning PBC, CKBC, and CBC adsorbents by soaking with deioned water

2. Characterizations of and Experiments on PBC, CKBC, and CBC adsorbents

2.1 Preparing a water sample for examining PZC

2.2 Shaking samples for PZC determination for 24 hours

2.3 Conducting adsorption kinetic experiment

2.4 Sampling the sample for adsorption kinetic study

2.5 Preparing water samples Preparing water samples for adsorption isotherm; effects of pH ,initial concentration, anions study; and desorption experiments

2.6 Adding BC adsorbents to synthetic water for adsorption isotherm; effects of pH ,initial concentration, anions study; and desorption experiments

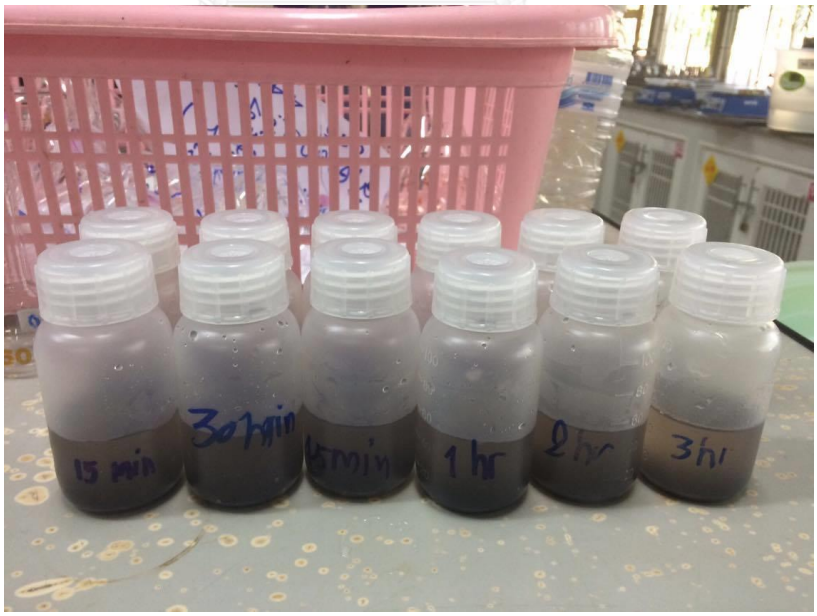

2.7 Shaking samples


2.8 Filtering samples after shaking



2.9 Samples after filtration (ready for analyses)

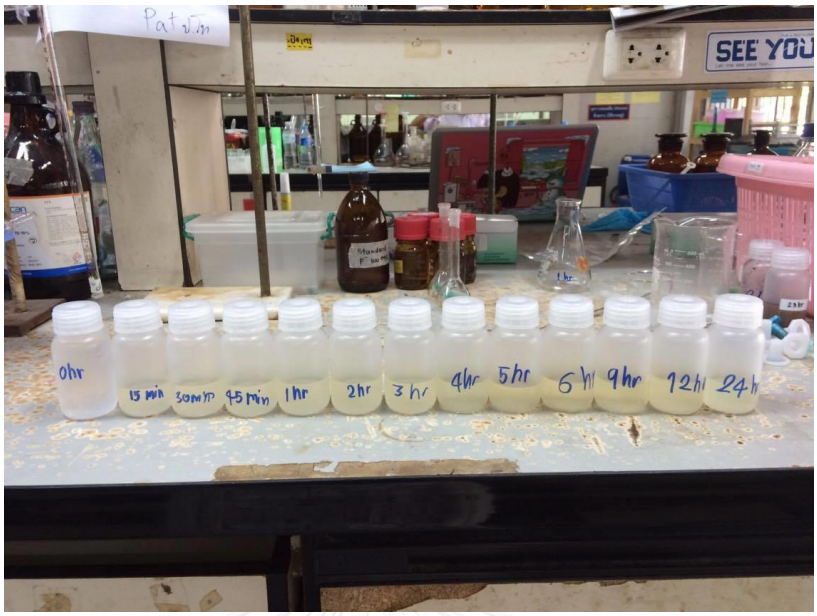

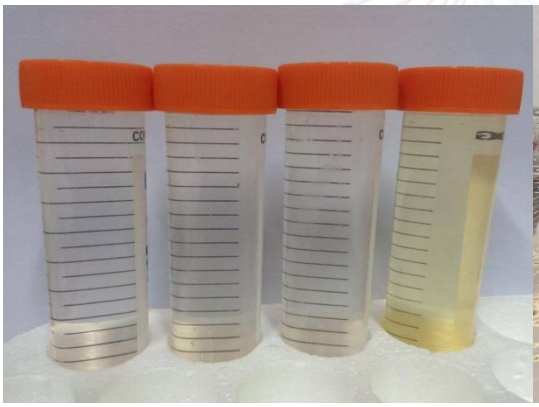

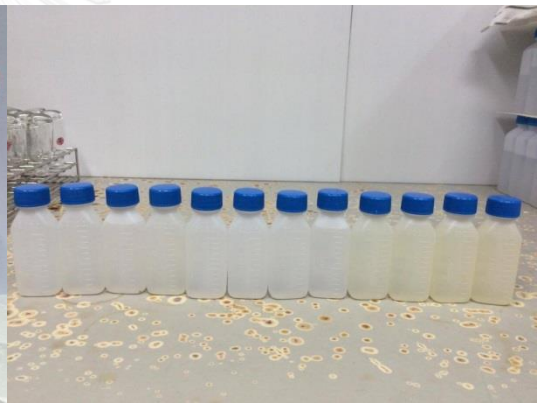

3. Analytical methods

3.1 Preparing water samples for fluoride analysis

3.2 Water samples after adding 10 mL of the SPADNS solution

3.3 Water samples after adding 1.0 mL of the indicator-acidifier reagent for chloride analysis

3.4 Water samples after titrating with 0.0141 N of Hg $(NO_3)_2$

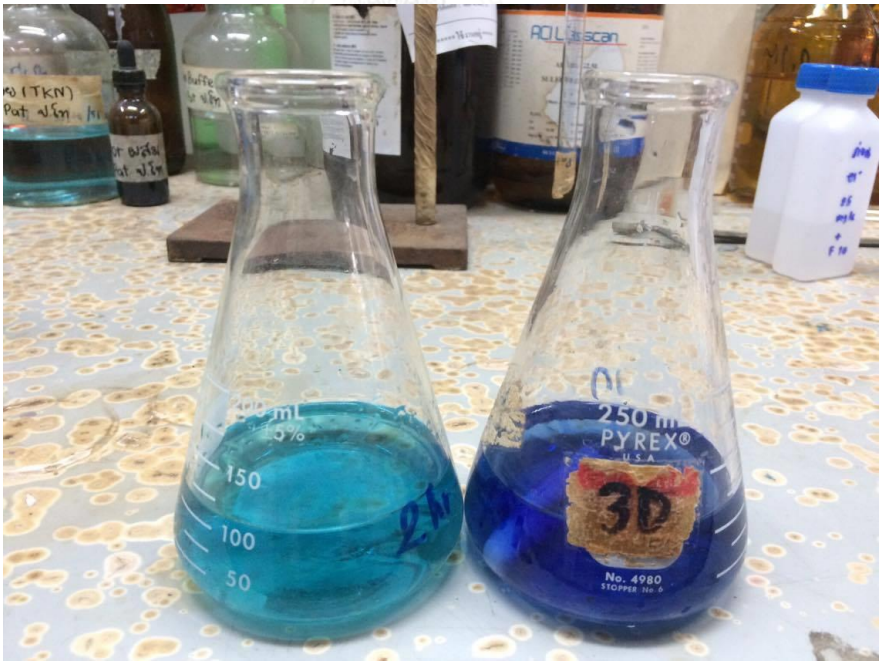

APPENDIX B
STANDARD CALIBRATION

Standard curve

1. Standard curve for fluoride analysis

A standard calibration curve was newly prepared for fluoride analysi for every batch of sample. It was applying the reference solution for setting the 0 mg/L of fluoride concentration. Thus, the fluoride concentration depended on the set reference solution. The standard calibration curve was a plot between absorbance values which obtained from a UV-Spectrophotometer (UV-6400 SPECTROPHOTOMETER, JENWAY), 570 nm and standard fluoride concentration (mg/L)

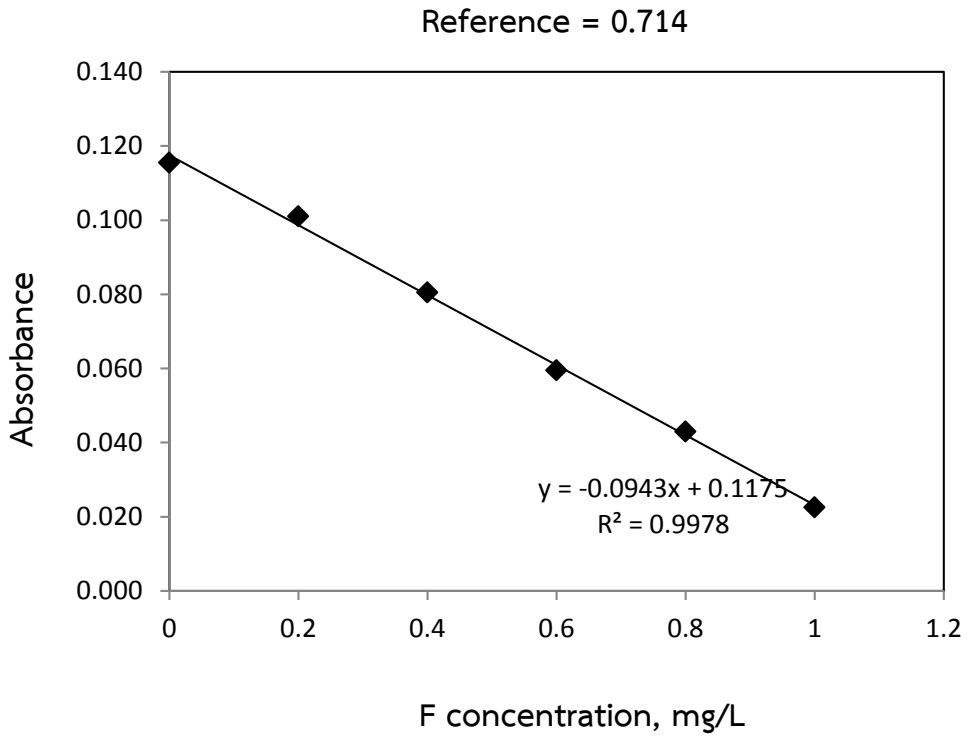

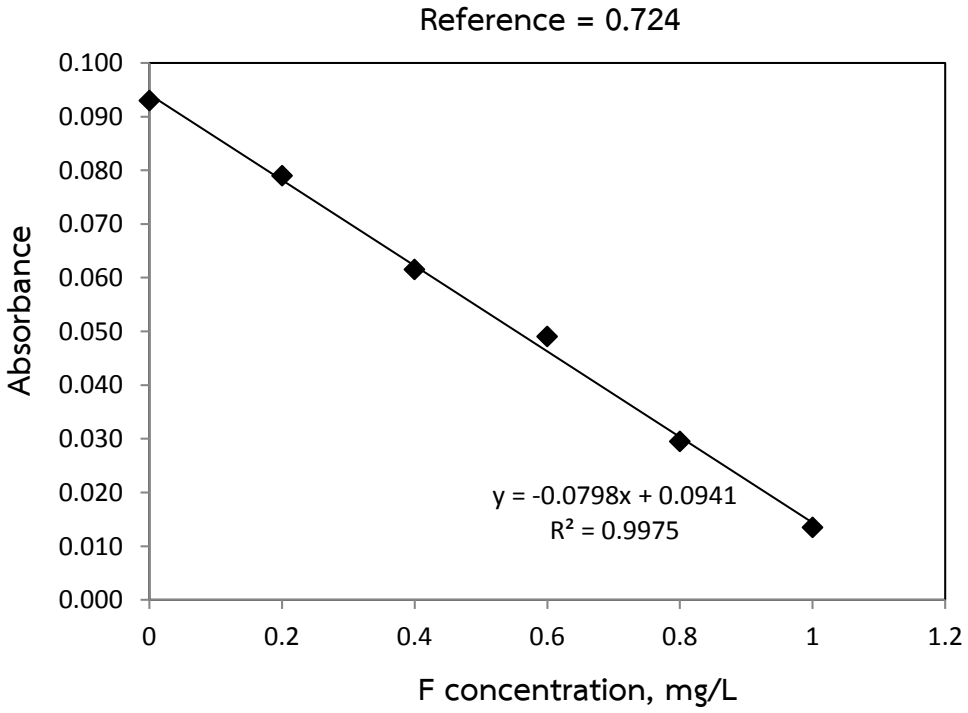
Reference = 0.724
Absorbance
0.100
0.090
0.080
0.070
0.060
0.050
0.040
0.030
0.020
0.010
0.000
0
0.2
0.4
0.6
0.8
1
1.2
y = -0.0798x + 0.0941
R² = 0.9975
F concentration, mg/L

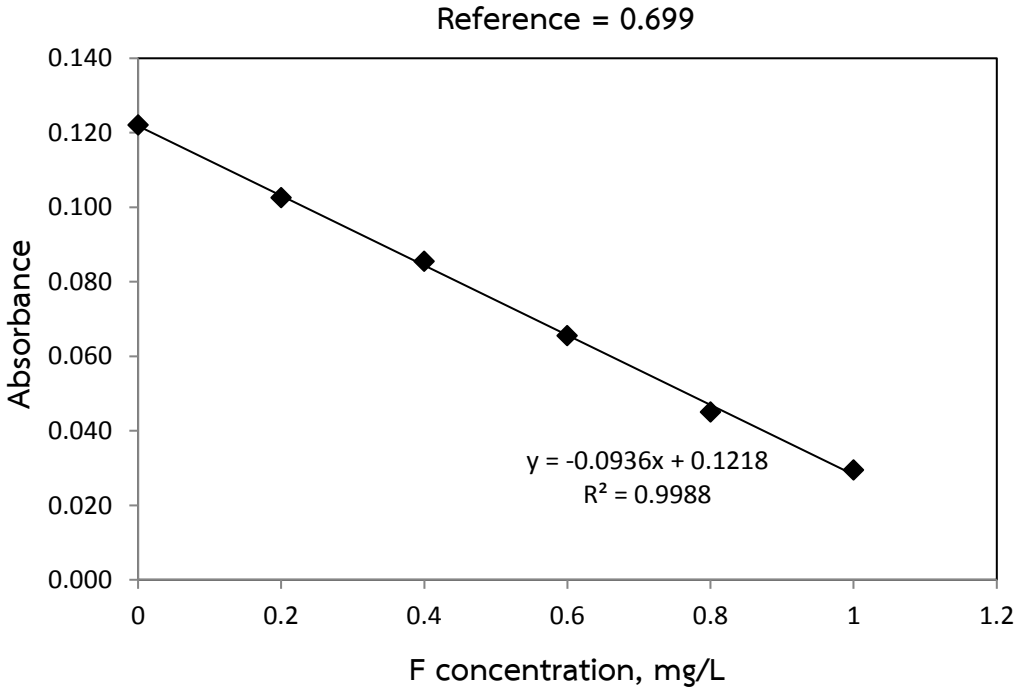
Reference = 0.699
Absorbance
0.140
0.120
0.100
0.080
0.060
0.040
0.020
0.000
0
0.2
0.4
0.6
0.8
1
1.2
y = -0.0936x + 0.1218
R² = 0.9988
F concentration, mg/L

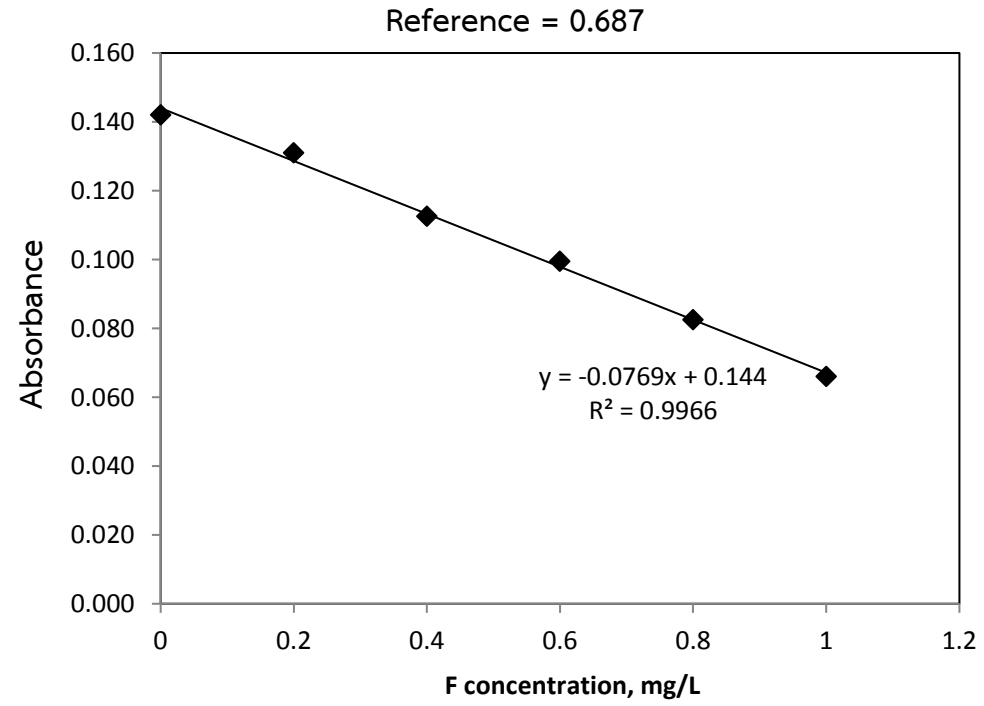
Reference = 0.687
Absorbance
0.160
0.140
0.120
0.100
0.080
0.060
0.040
0.020
0.000
0
0.2
0.4
0.6
0.8
1
1.2
y = -0.0769x + 0.144
R² = 0.9966
F concentration, mg/L

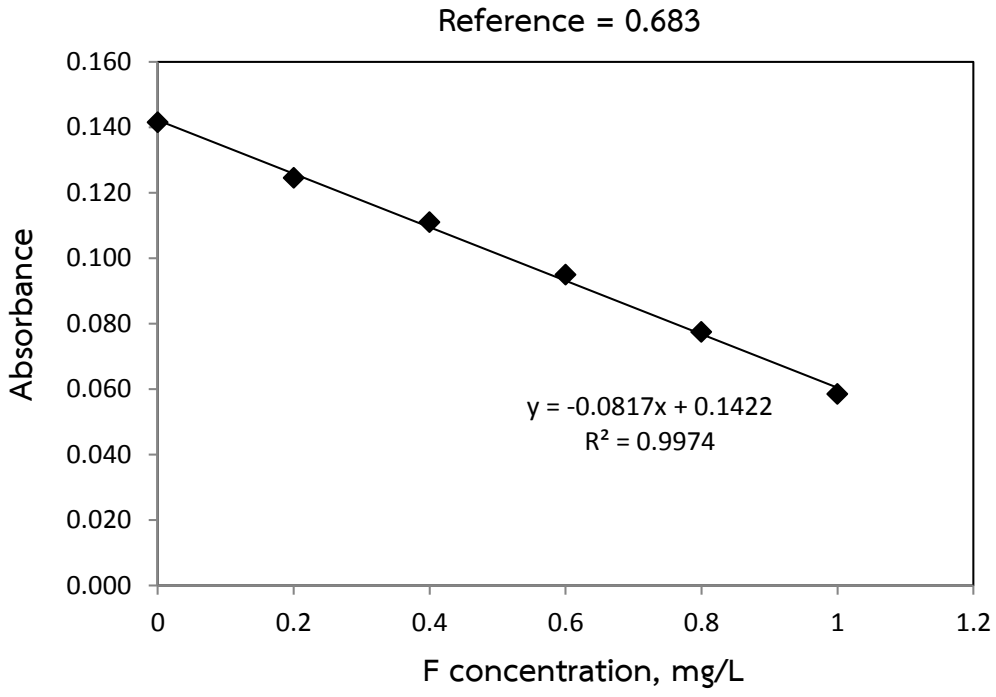
Reference = 0.683
Absorbance
0.160
0.140
0.120
0.100
0.080
0.060
0.040
0.020
0.000
0
0.2
0.4
0.6
0.8
1
1.2
y = -0.0817x + 0.1422
R² = 0.9974
F concentration, mg/L

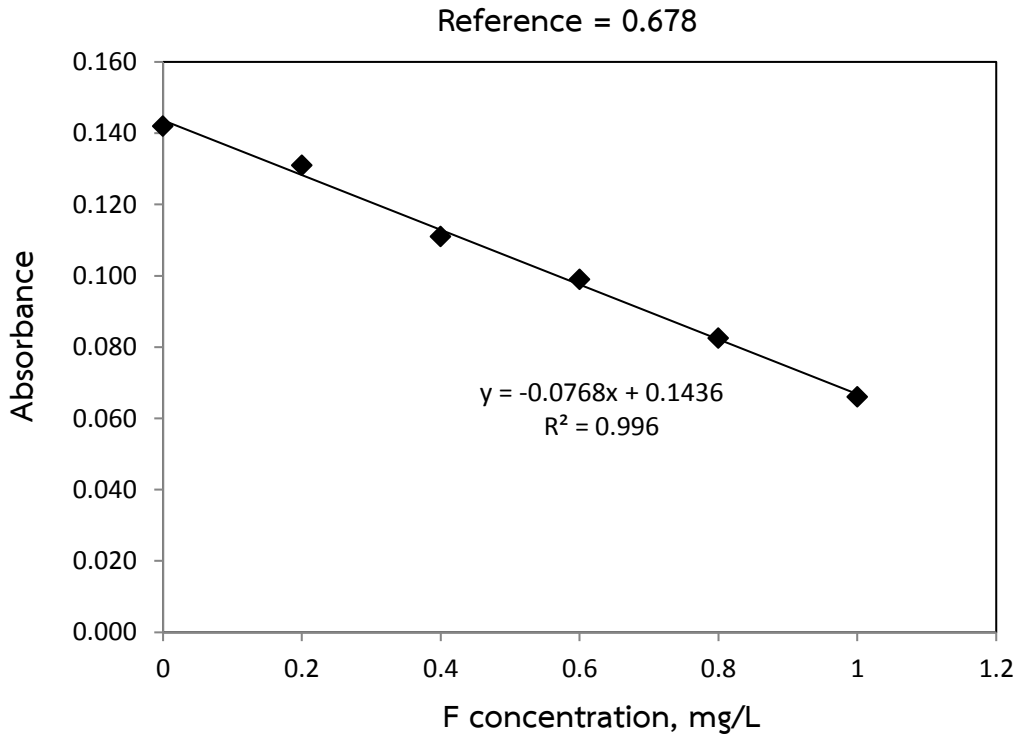
Reference = 0.678
Absorbance
0.160
0.140
0.120
0.100
0.080
0.060
0.040
0.020
0.000
0
0.2
0.4
0.6
0.8
1
1.2
y = -0.0768x + 0.1436
R² = 0.996
F concentration, mg/L

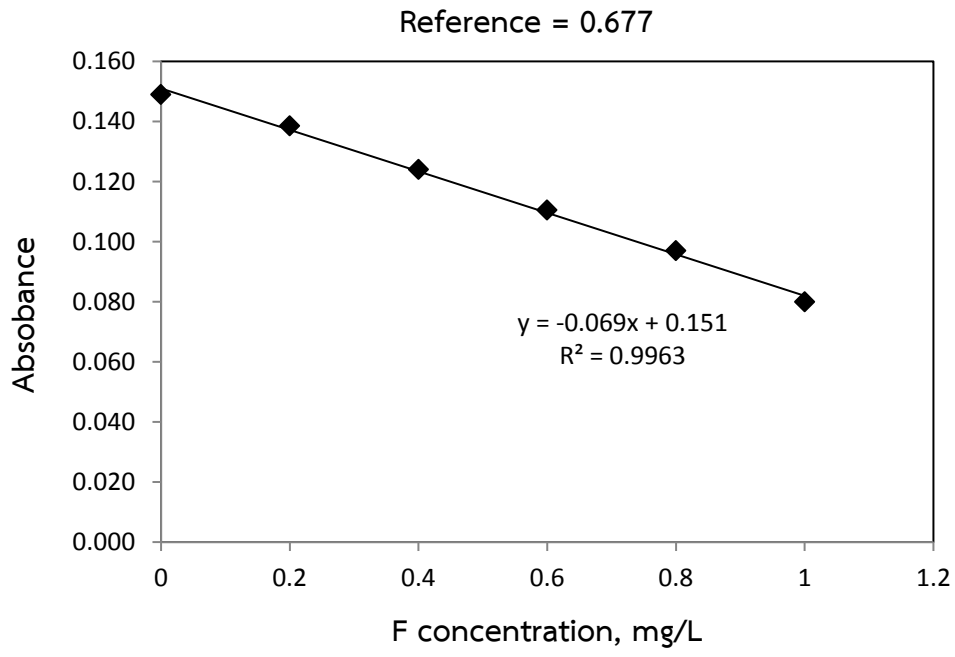
Reference = 0.677
Absobance
0.160
0.140
0.120
0.100
0.080
0.060
0.040
0.020
0.000
0
0.2
0.4
0.6
0.8
1
1.2
y = -0.069x + 0.151
R² = 0.9963
F concentration, mg/L

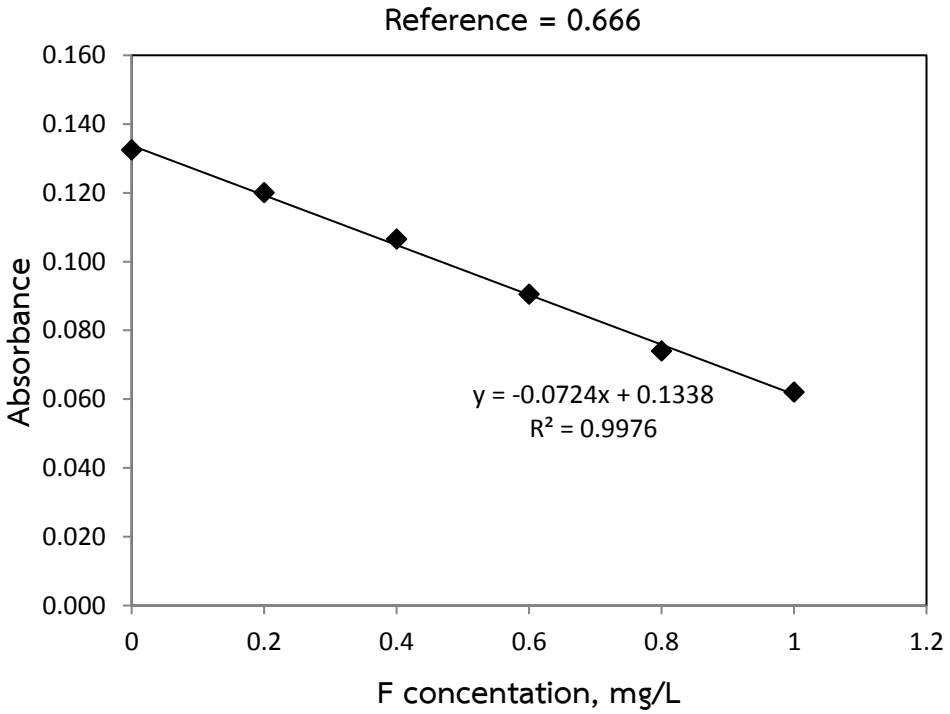
Reference = 0.666
Absorbance
0.160
0.140
0.120
0.100
0.080
0.060
0.040
0.020
0.000
0
0.2
0.4
0.6
0.8
1
1.2
y = -0.0724x + 0.1338
R² = 0.9976
F concentation, mg/L

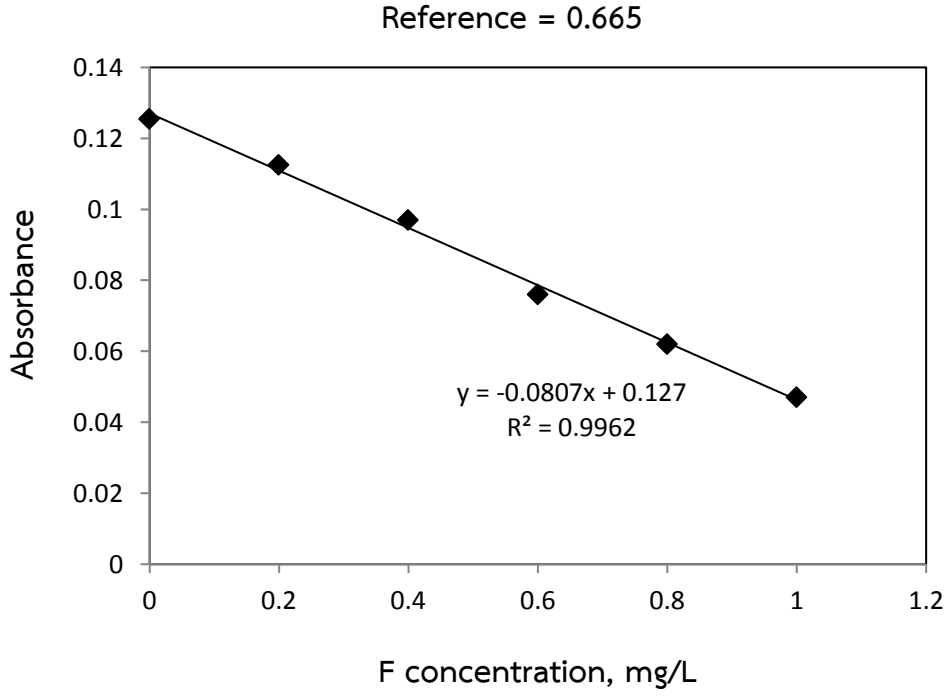
Reference = 0.665
Absorbance
0.14
0.12
0.1
0.08
0.06
0.04
0.02
0
0
0.2
0.4
0.6
0.8
1
1.2
y = -0.0807x + 0.127
R² = 0.9962
F concentration, mg/L

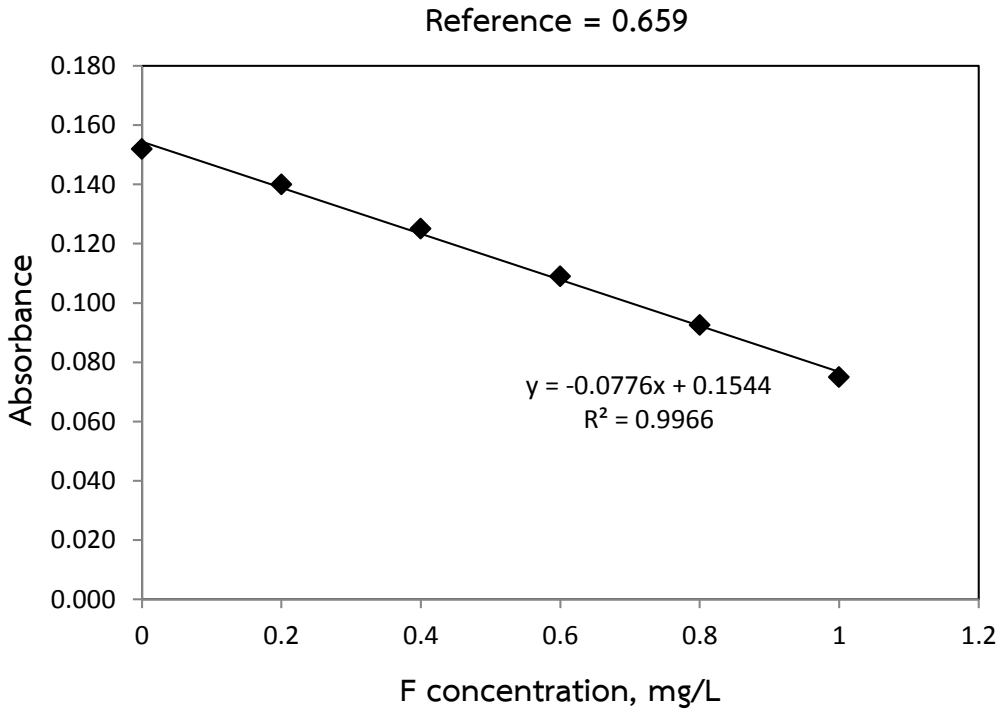
Reference = 0.659
Absorbance
0.180
0.160
0.140
0.120
0.100
0.080
0.060
0.040
0.020
0.000
0
0.2
0.4
0.6
0.8
1
1.2
y = -0.0776x + 0.1544
R² = 0.9966
F concentration, mg/L

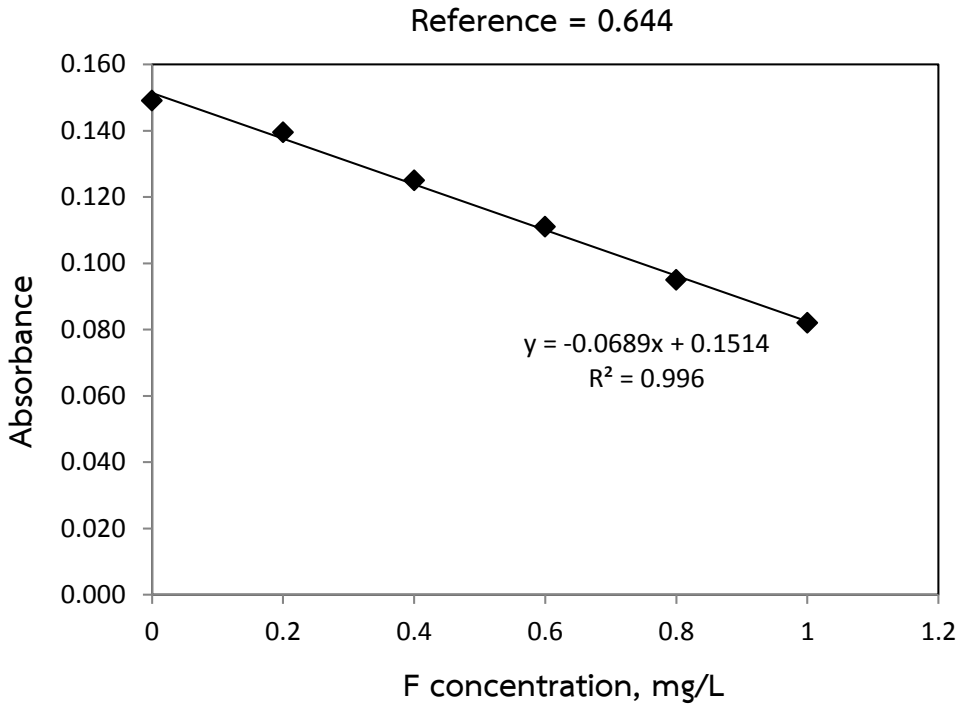
Reference = 0.644
Absorbance
0.160
0.140
0.120
0.100
0.080
0.060
0.040
0.020
0.000
0
0.2
0.4
0.6
0.8
1
1.2
y = -0.0689x + 0.1514
R² = 0.996
F concentration, mg/L

2. Standard curve for sulfate analysis

Standard curve was plotted between absorbance value and sulfate concentration (µg).

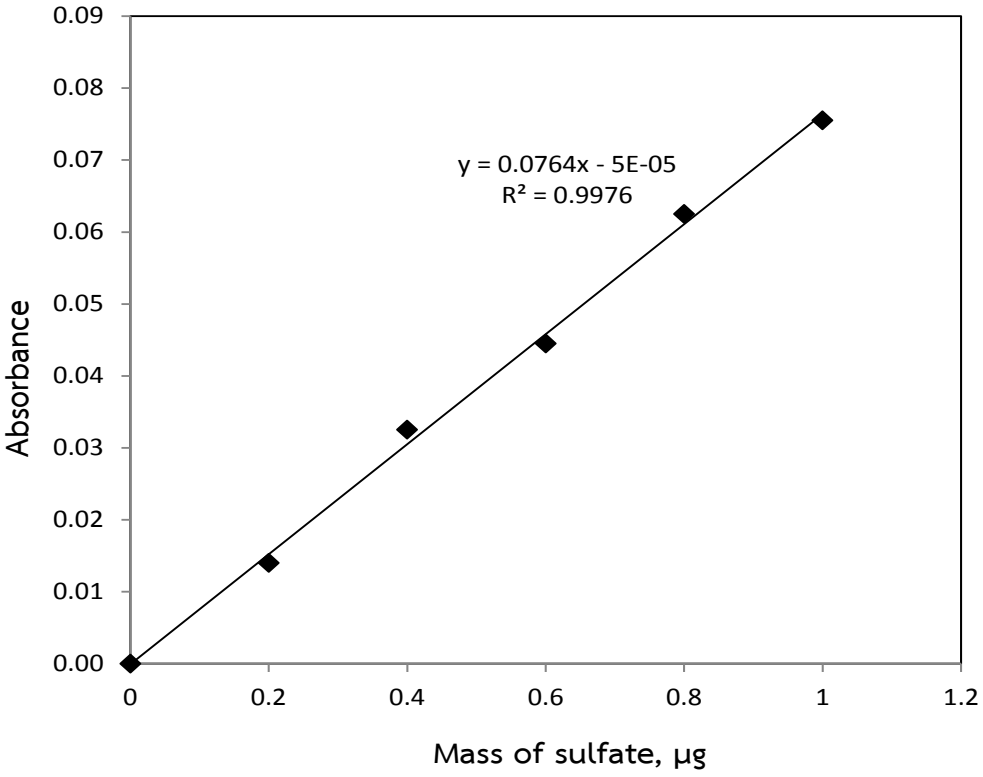

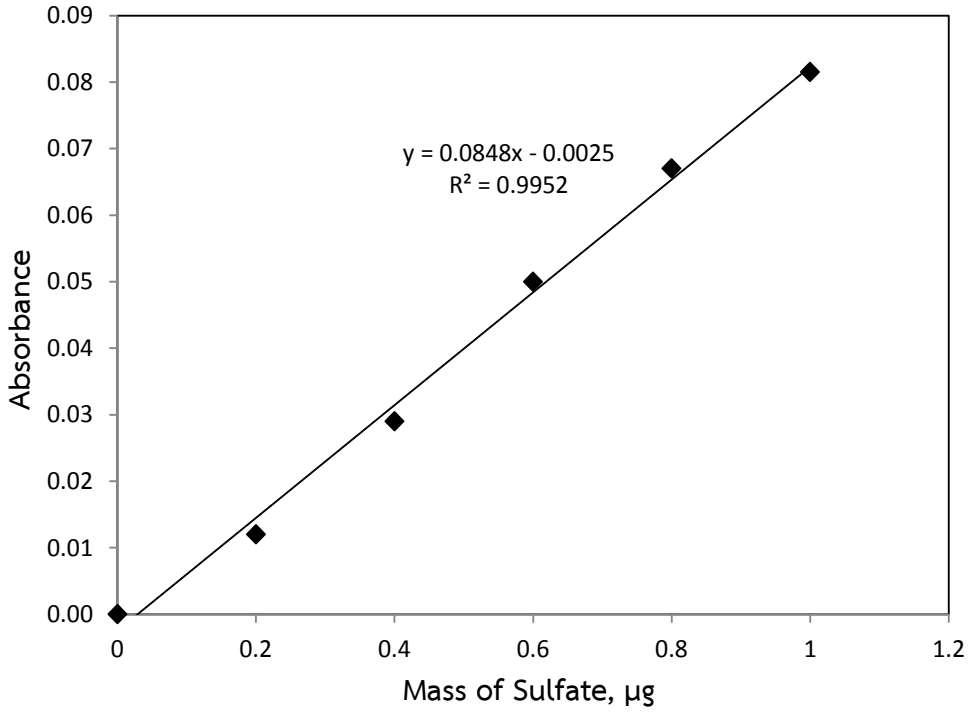

APPENDIX C
EXPERIMENTAL DATAS

1. Percentage of HAP based on XRD data

Charring condition		% HAP		
Temperature ℃	Retention time, h	PBC	CKBC	CBC
105	24	57.221	56.219	47.09
450	1	60.624	63.476	41.894
	2	52.948	70.225	61.959
	3	71.016	65.29	54.289
550	1	63.258	67.242	51.647
	2	77.588	77.692	54.26
	3	70.414	71.168	63.128
650	1	71.727	67.816	54.63
	2	68.578	75.581	53.382
	3	92.837	85.287	58.324

2. Point of zero charge data

Initial pH solution	Final pH solution		
	PBC	CKBC	CBC
3.093	6.811	6.948	6.851
4.949	8.219	8.514	7.811
7.172	8.581	8.910	7.876
9.029	8.761	9.0323	8.001
11.003	10.412	10.550	10.242
12.023	11.340	11.457	11.435

3. Adsorption kinetic data

Time, min	q_t of fluoride, mg/L		
	PBC	CKBC	CBC
0	0.000	0.000	0.00
5	0.310	0.256	0.379

10	0.335	0.281	0.362
20	0.386	0.247	0.337
30	0.428	0.384	0.455
60	0.371	0.309	0.400
120	0.384	0.206	0.435
180	0.384	0.212	0.435
360	0.372	0.212	0.435
540	0.324	0.243	0.356
720	0.443	0.325	0.527
1440	0.449	0.337	0.521

4. Adsorption isotherm data

Initial F, mg/L			Final F, mg/L			q_e of fluoride, mg/g		
PBC	CKBC	CBC	PBC	CKBC	CBC	PBC	CKBC	CBC
2.917	2.598	2.174	1.474	2.545	1.1	0.072	0.003	0.053
4.306	4.03	3.659	1.528	2.333	1.474	0.138	0.085	0.109
5.855	5.673	5.514	2.917	2.439	1.635	0.146	0.161	0.193
7.991	7.794	7.423	2.115	3.181	2.222	0.292	0.23	0.259
10.321	9.968	9.65	2.735	3.393	3.376	0.377	0.327	0.312
12.137	12.195	11.241	2.628	4.348	2.949	0.474	0.39	0.412
13.739	12.937	12.937	3.483	3.606	2.735	0.511	0.463	0.506
16.09	14.74	14.528	3.269	3.924	3.59	0.635	0.538	0.544

5. Effect of solution pH on adsorption capacity data

Initial pH of solution			Final pH of solution			q_e of fluoride, mg/g		
PBC	CKBC	CBC	PBC	CKBC	CBC	PBC	CKBC	CBC
4.004	4.004	4.004	7.123	7.136	7.113	0.33	0.132	0.166
5.994	6.003	6.003	7.186	7.158	7.173	0.366	0.153	0.187
8.618	9.035	8.014	8.336	8.288	8.016	0.134	0.113	0.072

10.005	10.014	10.014	8.436	8.461	8.248	0.079	0.089	0.085
12.003	12.004	12.004	10.683	10.986	10.531	0.037	0.083	0.096

6. Effect of chloride ion on adsorption capacity data

Initial F concentration, mg/L	Final F concentration, mg/L		
	PBC	CKBC	CBC
13.941	9.449	11.927	8.209
21.375	8.674	10.843	5.886
83.024	29.74	24.783	13.631
97.893	43.371	42.131	14.87

7. Effect of sulfate ion on adsorption capacity data

Initial Cl ,mg/L	Initial F , mg/L	Final F concentration, mg/L			q_e of fluoride ,mg/g		
		PBC	CKBC	CBC	PBC	CKBC	CBC
9.018	36.512	25.262	32.609	25.362	0.557	0.195	0.557
25.928	36.277	26.087	33.623	27.101	0.513	0.137	0.463
51.856	36.522	26.087	33.333	30.725	0.519	0.159	0.289

8. Desorption data

Initial sulfate ,mg/L	Initial F, mg/L	Final F concentration, mg/L			q_e of fluoride ,mg/g		
		PBC	CKBC	CBC	PBC	CKBC	CBC
19.136	36.142	26.464	27.845	25.359	0.482	0.413	0.538
42.173	36.845	27.431	29.227	26.326	0.469	0.379	0.522
64.948	36.000	28.812	29.503	25.774	0.359	0.324	0.501

9. Data of Desorption process

pH solution of desorption process			F desorbed, mg/L		
PBC	CKBC	CBC	PBC	CKBC	CBC
6.003	6.003	6.003	1.733	2.152	1.699
8.619	9.075	8.068	2.088	1.798	1.733
11.021	11.021	11.021	8.563	8.144	7.629

VITA

Miss Benyapa Sawangjang was born on August 16, 1991 in Chiang Mai province. She graduated Bachelor's degree of Engineering from Department of Environmental Engineering, the Faculty of Engineering, Chiang Mai University in 2013. She continues studied Master degree in the International Program in Environmental Management, Chulalongkorn University in 2014.